Report No.: NIH/TR/2020-21/SWHD/**

DEVELOPMENT OF REGIONAL RELATIONSHIPS FOR WATER AVAILABILITY ANALYSIS AND FLOOD ESTIMATION FOR LOWER GODAVARI BASIN (3F)

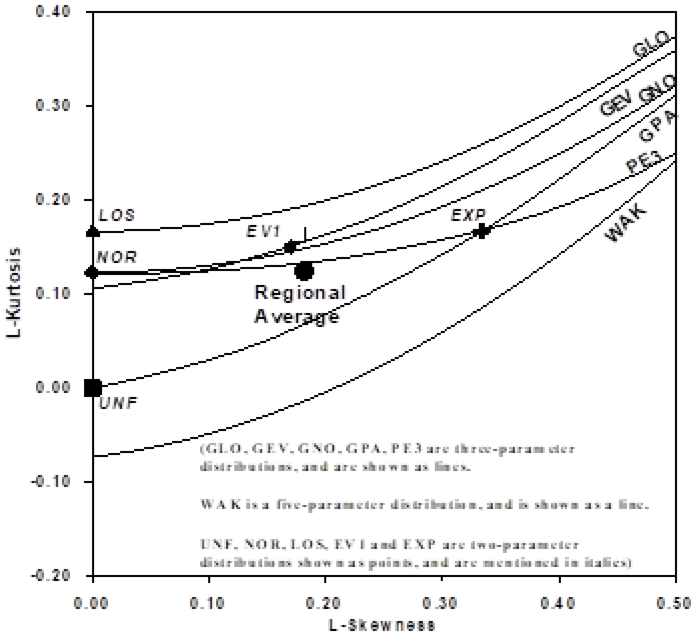

NATIONAL INSTITUTE OF HYDROLOGY

राष्ट्रीय जलविज्ञान संस्थान

आपो हि ष्ठा मयोभुवः

National Institute of Hydrology

Department of WR, RD & GR,
Ministry of Jal Shakti, Govt. of India
Jal Vigyan Bhawan, Roorkee - 247667 (Uttarakhand), INDIA

March 2021

FINAL REPORT

Report No.: NIH/TR/2020-21/SWHD/**

DEVELOPMENT OF REGIONAL RELATIONSHIPS FOR WATER AVAILABILITY ANALYSIS AND FLOOD ESTIMATION FOR LOWER GODAVARI BASIN (3F)

आपो हि ष्ठा मयोभुवः

National Institute of Hydrology
Department of WR, RD & GR,
Ministry of Jal Shakti, Govt. of India
Jal Vigyan Bhawan, Roorkee - 247667 (Uttarakhand), INDIA

March 2021

DIRECTOR: Dr. J. V. Tyagi

Division: Surface Water Hydrology Division (SWHD)

Head: Dr. Rakesh Kumar, Scientist ‘G’

Principal Investigator: Dr. Sanjay Kumar, Scientist ‘E’

Study Team:

Dr. Rakesh Kumar Sc G (Co-PI)

Dr. Pankaj Mani, Sc E; (Co-PI)

Er. J. P. Patra, Sc C; (Co-PI)

CONTENTS

PREFACE

This report presents a comprehensive hydrological assessment integrating regionalization techniques and frequency analysis methods to improve the understanding of water resources variability and extremes. The study focuses on two main objectives i.e. (i) Developing regional relationships for (surface) water availability analysis and (ii) Development of at site and regional flood frequency analysis using L Moments. Additionally, the study also investigates the (a) Development of at site and regional rainfall frequency analysis using L moments, (b) Development of regional relationships for Nash and Clark IUH models parameters and (c) Impact of climate change on flood estimates. Together, these components provide a robust framework for analyzing hydrological behavior across ungauged and sparsely gauged basins.

Regionalization of FDCs plays a crucial role in estimating flow characteristics at ungauged locations by transferring information from hydrologically similar basins. This approach supports water resource planning, ecological flow assessment, and drought management. Complementing this, the application of L-moment-based regional flood frequency analysis ensures reliable estimation of design floods by addressing data limitations and reducing the influence of outliers. The use of L-moments provides a statistically robust alternative to conventional moment methods, particularly for heterogeneous hydrological regions.

The report further explores extreme rainfall frequency analysis using L-moments, which is essential for understanding precipitation extremes and their implications for flood risk, infrastructure design, climate resilience and supports improved hydrological modeling. In addition, the regionalization of Clark and Nash GIUH models is undertaken to derive unit hydrographs based on basin geomorphology. This enables the estimation of runoff responses in ungauged catchments, contributing to efficient watershed management and flood estimation. The inclusion of trend analysis of annual maximum floods provides insights into the impacts of climatic variability and land-use changes on flood behavior over time.

Overall, this report aims to integrate advanced statistical and hydrological techniques to support sustainable water resources management. The findings are expected to be valuable for researchers, engineers, and policymakers engaged in hydrological planning, risk assessment, and climate adaptation strategies. The study group includes Sanjay Kumar, Sc E; Rakesh Kumar, Sc G; J. P. Patra, Sc C and Pankaj Mani, Sc E.

EXECUTIVE SUMMARY

This report presents a comprehensive hydrological investigation focusing on regionalization techniques and frequency analysis methods to improve the estimation of hydrological variables in both gauged and ungauged basins. The study is structured to address key components in a systematic manner, beginning with the regionalization of Flow Duration Curves (FDCs), followed by regional flood frequency analysis using L-moments, extreme rainfall frequency assessment, regionalization of geomorphological unit hydrographs, and concluding with trend analysis of annual maximum floods.

The first component of the study examines various approaches for the regionalization of Flow Duration Curves, emphasizing their importance in estimating streamflow characteristics where observed data are limited or unavailable. Three distinct methods are evaluated, including regionalization of distribution parameters at individual sites, regionalization at the basin scale, and direct regionalization of dependable flows. Given that many practical water resource applications require only specific dependable flows rather than the entire FDC, the study prioritizes the regionalization of flows corresponding to selected exceedance probabilities. Using hydrological and physiographic data from multiple gauging sites in the lower Godavari basin, empirical relationships are developed for flows corresponding to different dependability levels. The results demonstrate that these regional relationships provide reasonably accurate flow estimates, thereby supporting their application in planning and design contexts .

The second part of the report focuses on regional flood frequency analysis using the L-moment approach. A rigorous data screening process is carried out using discordancy measures, followed by homogeneity testing based on L-moment statistics. The analysis identifies a homogeneous group of catchments suitable for regional modeling. Several probability distributions are evaluated using L-moment ratio diagrams and statistical goodness-of-fit measures. Among these, the Generalized Extreme Value (GEV) distribution is found to provide the most reliable representation of flood behavior in the study region. Regional relationships are then developed to estimate floods for various return periods, both for gauged and ungauged catchments, by linking flood characteristics with basin attributes such as catchment area. This approach enhances prediction reliability while reducing uncertainty associated with limited data availability .

The study also incorporates an analysis of extreme rainfall using L-moments, recognizing the growing importance of precipitation extremes under changing climatic conditions. Variations in rainfall intensity, frequency, and distribution are assessed in the context of increasing atmospheric temperatures and greenhouse gas concentrations. These changes have significant implications for flood generation processes and water resource systems, particularly in vulnerable regions. The regional frequency analysis of rainfall extremes supports improved estimation of design rainfall and contributes to more resilient infrastructure planning and flood risk management strategies .

Another important aspect of the report is the regionalization of the Geomorphological Instantaneous Unit Hydrograph (GIUH) based on Clark and Nash models. The GIUH approach utilizes catchment geomorphological characteristics derived through GIS tools to estimate runoff response. The developed model is applied to multiple rainfall-runoff events, and its performance is evaluated against observed hydrographs as well as established hydrological models. The results indicate that the GIUH-based approach is capable of simulating direct surface runoff with satisfactory accuracy, making it particularly useful for ungauged basins where conventional calibration is not feasible.

Finally, the report investigates trends in annual maximum flood series to assess the influence of climatic variability and large-scale atmospheric phenomena. Both parametric and non-parametric statistical methods are applied to detect trends over long-term data records. While the results indicate no statistically significant trends at the chosen confidence level, the analysis provides valuable insights into the variability of flood behavior. Additionally, the relationship between annual maximum floods and climate indices such as the El Niño–Southern Oscillation (ENSO) is explored to improve understanding of flood predictability.

Overall, the study integrates regionalization techniques, L-moment-based statistical methods, and geomorphological modeling to develop reliable tools for hydrological analysis. The findings contribute to improved estimation of hydrological extremes and support effective water resources planning, infrastructure design, and risk management in data-scarce regions.

CHAPTER 1

REGIONAL RELATIONSHIPS FOR WATER AVAILABILITY ANALYSIS

1. INTRODUCTION

Information about stream flow characteristics (such as catchment yield, peak discharge, low flows etc.) are required for planning and management of water resources. The temporal variability of these characteristics evaluated as frequency of occurrence or return period provides inputs for the safe and cost effective engineering design of projects/hydraulics structures. The flow duration curve has been identified as one of the most important descriptor of stream flow variability and find number of applications in engineering hydrology (Foster, 1934; Barrows, 1943; Searcy, 1959; Chow, 1964; Riggs, 1982; Gupta, 1989). A Flow Duration Curve (FDC) is a graphical representation of the relationship between a given stream discharge and the percentage of time this discharge is equalled or exceeded and it is an important signature of the hydrologic response of the catchment. The FDCs may be easily developed for sites having adequate records of stream flow however, for ungauged sites or sites having inadequate flow data the regional flow duration curves are developed and utilized for the estimation of available water resources (Mimikou and Kaemaki, 1985; Fennessey and Vogel, 1990; Krasovskaia et al., 2006; Pugliese et al., 2016).

Development of regional relationships for the prediction of the FDC in (partially) gauged and ungauged basins has been an area of active hydrological research for years (Singh, 1971; Fennessey and Vogel, 1990; Castellarin et al., 2013). The International Association of Hydrological Science (IAHS) also launched an initiative for Prediction in Ungauged Basins (PUB) (Sivapalan et al. 2003) because of widespread use of prediction of FDCs in water resources engineering. Regional model proposed in the literature follow a variety of different approaches and conceptualization. These has been detailed by Castellarin et al. (2013, 2004). Dimensionless flow duration curve (DFDC) provides a starting point for regionalization of the FDC. For regionalization two step approach is utilized i.e. identification of homogeneous regions and use of multiple regression. Size of the basin and length of the main river are generally used in regression (Krasovskaia, et al., 2006). This indicates the dependence of the FDC on spatial scale, an aspect that will be further explored in the paper. Fennessey and Vogel, (1990) employed regional regression to predict daily FDC in ungauged basin. Farmer et al. (2014) also employed regional multiple regression to predict an estimate of the logarithmically transferred quantiles as a function of basin characteristics. Geostatistical techniques were also employed to predict stream flow indices in ungauged basins (Castiglioni et al. 2009; Archfield et al. 2013). Such techniques use kriging methods and do not require identification of homogeneous regions.

Regional regression is one of the most common used techniques for the prediction of FDCs at ungauged sites (Castellarin et al., 2013; Farmer and Vogel, 2013). At its simplest, regional regression treats the continuous FDC as discrete points. Farmer et al. (2014) discretise the FDC into 27 quantiles, with duration of 0.02, 0.05, 0.1, 0.2, 0.5, 1, 2, 5, 10, 20, 25, 30, 40, 50, 60, 70 75, 80, 90, 95, 98, 99, 99.5, 99.8, 99.9, 99.95 and 99.98 percent and a log-linear regression model was developed for each duration using a range of basin characteristics. This study, also uses regional regression to predict flows corresponding to different duration. The methodology used is described below along with the other commonly used techniques for regionalization of flow duration curve.

2. LITERATURE REVIEW

The development of regionalization techniques for FDCs has evolved over time, with early studies focusing on statistical and regression-based approaches. These methods establish empirical relationships between FDC characteristics, such as flow quantiles, and catchment descriptors including drainage area, precipitation, slope, and land use. Regression-based models remain among the most widely applied techniques due to their simplicity and ease of implementation. Studies have demonstrated that while simple models based on drainage area can provide initial estimates, incorporating multiple physiographic and climatic variables significantly improves predictive performance (Yu et al., 2002; Li et al., 2010).

Another important class of regionalization methods is the index flow or dimensionless curve approach. In this framework, observed FDCs are normalized using a characteristic flow parameter, typically the mean or median flow, to produce dimensionless curves. These normalized curves are assumed to be similar within a homogeneous region and can be scaled using the index flow to estimate site-specific FDCs. Castellarin et al. (2004) demonstrated the effectiveness of this approach when combined with appropriate regionalization of the index flow parameter.

The identification of homogeneous regions is a critical prerequisite for successful regionalization. Cluster analysis and catchment classification techniques are widely employed to group basins based on similarity in hydrological response, climatic conditions, and physiographic characteristics. Studies have shown that regionalization performance improves significantly when catchments are classified into homogeneous groups prior to model development (Yadav et al., 2007; Boscarello et al., 2015).

Parametric approaches represent another important category of FDC regionalization techniques. These methods involve fitting theoretical probability distributions, such as lognormal, exponential, or generalized Pareto distributions, to observed FDCs and subsequently regionalizing the parameters of these distributions. Parametric models provide smooth and continuous representations of FDCs and are particularly useful for extrapolation. However, their effectiveness depends on the flexibility of the chosen distribution to capture the variability of flow regimes across different catchments (Sadegh et al., 2016).

In addition to parametric methods, non-parametric approaches have also been developed to estimate FDCs without assuming a predefined functional form. These methods rely on empirical relationships and data-driven techniques to estimate flow quantiles directly. Ganora et al. (2009) introduced a non-parametric framework for regionalizing FDCs in ungauged basins. Similarly, geostatistical approaches such as Top-kriging have been applied to estimate FDCs by interpolating flow characteristics across spatially distributed catchments (Pugliese et al., 2016).

The shape of FDCs is strongly influenced by climatic and physiographic factors, including precipitation patterns, evapotranspiration, geology, and catchment storage characteristics. Climate seasonality plays a particularly important role, as regions with pronounced wet and dry seasons tend to exhibit steep FDCs reflecting high variability in streamflow. Geological characteristics, such as permeability and groundwater storage capacity, influence baseflow contributions and thus affect the low-flow portion of the curve (Cheng et al., 2012; Ye et al., 2012).

Despite significant advancements, several challenges remain in the regionalization of FDCs. Data scarcity continues to be a major limitation, particularly in regions with limited hydrological observations. In addition, uncertainties associated with model structure, parameter estimation, and input data can significantly affect the reliability of regional predictions. Castellarin et al. (2004) emphasized the importance of using validation techniques such as jackknife and bootstrap methods to assess model robustness. Another challenge is the transferability of regional models across different regions, as models developed in one climatic or physiographic setting may not perform well in others.

Recent research indicates a growing interest in integrating process-based understanding with statistical approaches to improve FDC regionalization. Hybrid methods that combine empirical relationships with hydrological insights are increasingly being explored. Furthermore, there is a growing recognition of the need to incorporate the impacts of climate variability and land-use change into regionalization frameworks, as these factors significantly influence streamflow regimes. Over time, methodologies have evolved from simple regression-based models to more sophisticated approaches incorporating clustering, parametric modeling, and geostatistical techniques. While considerable progress has been made, challenges related to data availability, uncertainty, and model transferability persist. Future research should focus on integrating physical process understanding with advanced statistical methods to develop more robust and reliable regionalization frameworks.

3. METHODOLGY

Numerous methods exist to predict specific stream flow statistics in ungaged basins (see Thomas and Benson, 1970, and Ries III, 2007, Bhunya et al. 2013, for a summary), however this section explains three commonly used methods for prediction of flows in ungauged catchments based on the available rainfall-runoff records for the gauged catchments of the region which is considered to be hydro-meteorologically homogeneous. These methods are explained below:

3.1 Regionalisation of the parameters of chosen probability distribution for individual gauged sites

Theoretically any distribution may be fitted to linearize the flow duration curve and best fit distribution may be chosen for further application. The parameters of the best fitted distribution may be estimated for the gauged catchments of the region and the regional relationships may be developed relating the distribution parameters with the physiographic and climatological characteristics of the basin. This involves developing the different relationships for the region using linear regression approach wherein the parameters of the distribution are considered as dependable variable (one at a time) and physiographic and/or climatological factors as independent variable(s). These relationships are then used to estimate the parameters of the selected distribution for the ungauged catchment

For example, if the normal distribution is fitted to develop the flow duration curve for gauged catchments of the region, the parameters $\overline{Q}$ and σ_Q may be related with their catchment characteristics. Typical forms of such equations for $\overline{Q}$ and σ_Q are given as:

$$\bar{Q} = C_1 logA \qquad (1)$$

$$\sigma_Q = C_2 + \frac{C_3}{H} \qquad (2)$$

where $\overline{Q}$ = mean of the flow series (parameter of normal distribution;

σ_Q = standard deviation of the flow series (parameter of normal distribution)

A = Catchment area,

H = Basin Relief, and

C_1,C_2,and C_3 = the constants.

These constants are evaluated using simple linear regression approach from the data of gauged catchments.

3.2 Regionalisation of the parameters of a chosen probability distribution derived for the region as a whole

Many times, either adequate flow records for gauged catchments are not available or number of gauged catchments are limited. This makes the development of regional flow duration curve using method explained in section 2.1 erroneous. Under these circumstances it is considered appropriate to make all the flow data values of individual sites non-dimensional by dividing it by the mean of the flow occurring at that site. The non-dimensionalised flow data series of all the gauged sites are clubbed together to provide a simple series representing the region. While clubbing them together, it is presumed that these non-dimensional flow series for each gauging site in the region is a sample drawn from the same population. A single series, thus obtained, for the region may be analysed and a chosen probability distribution may be fitted. It results in the parameters of the distribution which may be considered as the regional parameters. These parameters may be used to get the non-dimensionalised flow for any level of dependability. In order to develop the flow duration curve for an ungauged catchment, the estimate for mean flow is required. It may be multiplied by the non-dimensional flow values for having the required flow duration curve. It necessitates the development of a regional relationship for the mean flow relating the values of the mean flows of the gauged catchments with their catchment characteristics as depicted in Eqn. (3) below.

$$\bar{Q} = a\, A^{b} \qquad (3)$$

where, $\bar{Q}$ = mean flow for different sites;

A = catchment area of the respective sites

a & b = constants for the region to be evaluated using linear regression approach.

3.3 Regionalisation of the dependable flows

The evaluation of dependable flows corresponding to the limited number of probability of exceedances does not requires to develop the complete flow duration curve for ungauged basin. In such situations the dependable flows itself may be regionalised rather than regionalising the flow duration curve. For the accuracy of this method adequate number of gauging sites having the flow series of the specific duration for a sufficiently long period are required. However, under the inadequate data situation method explained either in section 2.1 or section 2.2 may be used to regionalise the flow duration curves. The forms of the typical regional relationships for 50% and 90% dependable flows are given below:

$$Q_{50} = a_1 A^{a2} H^{a3} \qquad (4)$$

$$Q_{90} = b_1 A^{b2} H^{b3} \qquad (5)$$

where, Q_{50} and Q_{90} are the 50% and 90% dependable flows respectively. A and H represent the catchment area and relief respectively. a_1,a_2,a_3,b_1,b_2,and b_3 are the constants to be evaluated by using linear regression approach.

4. STUDY AREA AND DATA

The discharge data of different gauging sites in lower Godavari basin is used for regionalization of dependable flows. Fig 1 shows the lower Godavari basin and locations of various CWC gauging sites (CWC 2014). Table 1 provides the details of the lower Godavari basin and its various rivers. The annual dependable flow data at different sites provided in the CWC report (2018) is considered for regional regression analysis. The average annual catchment rainfall is also considered wherever it is available. Table 2 provides the descriptive statistics and other details of the data for 14 gauging sites in the lower Godavari basin.

Table 1: Details of Lower Godavari basin

Name of River	Elevation of Source (MSL)	Length (km)	Catchment Area (sq km)	Aver.Annual Rainfall (mm)
Lower Godavari (Pranhita Confluence to Sea)	107	462	24869	1208
Indravati	914	535	41655	1588
Sabari	1372	418	20427	1433

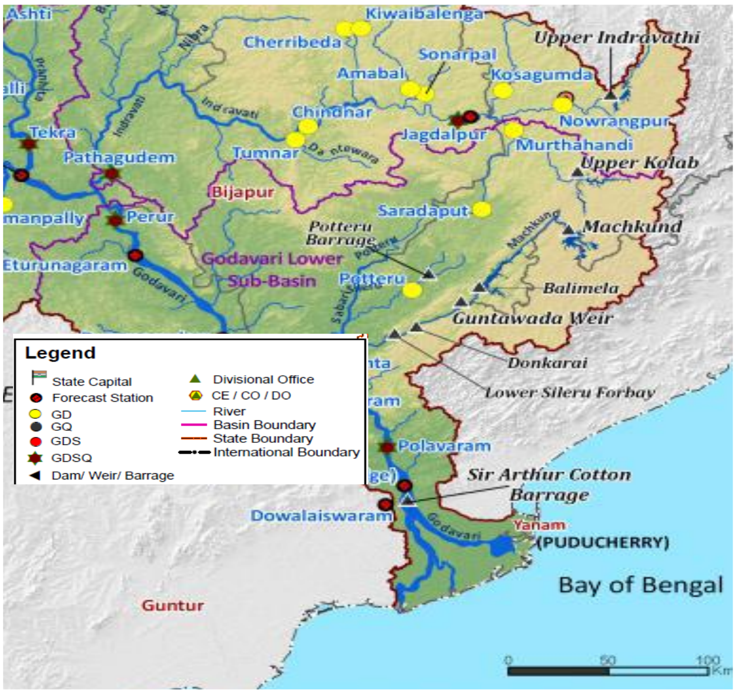

Fig. 1: Lower Godavari Basin (CWC Report, 2014)

Table 2: Statistics of annual flows at 14 sites, catchment area and annual rainfall

S.N.	Site Name	Mean (MCM)	SD	CV	Skew	Catchment Area (A) Km2	Catchment Annual Rainfall (mm)
1	Ambabal	849.50	331.62	0.39	0.94	1968	1387
2	Cherribeda	777.60	389.01	0.50	0.52	890	1387
3	Chindnar	9240.40	3392.61	0.37	0.21	17270	1450
4	Perur	75833.70	36921.64	0.49	0.64	268200	1015
5	Polavaram	89271.40	38364.77	0.43	0.03	307800	1082
6	Sangam	255.70	135.53	0.53	0.51	1565	1015
7	Saradaput	5202.70	1703.26	0.33	0.00	3047	1700
8	Sonarpal	702.50	226.50	0.32	0.43	1523	1433
9	Tumnar	1328.90	532.74	0.40	-0.06	1700	1450
10	Bhadrachalam	71501.0	37896.26	0.53	0.99	280505	1150
11	Somanpally	1112.50	850.60	0.76	0.63	12691	-
12	Pathagudem	24896.30	9317.51	0.37	0.21	40000	-
13	Konta	16491.70	5196.24	0.32	-0.57	19550	-
14	Kosagumda	1164.30	598.07	0.51	2.0	1635	-

5. RESULTS AND DISCUSSION

Regional regression relationships are developed considering data given in Table 2. The catchment area and annual catchment rainfall are considered as independent variables, whereas dependable flow corresponding to different probability of exceedance (CWC Report, 2018) are considered as dependent variable as explained in section 2.3. A total of 14 sites has been considered for developing regional regression relationships for the dependable flows corresponding to 10%, 25%, 50 % 75% and 90%. Data from first nine gauging sites in the table are utilized for developing the regional dependable relationships. The data of the last five sites has been used for validation. An investigation of dependable variable (Q_p) and explanatory variable (catchment area (A) and rainfall (P)) shows that catchment area captures the variation in dependable flows corresponding to different probability of exceedance compared to normal catchment rainfall. However, both the explanatory variables together explain the variation in the dependable flows better compared to catchment area alone. Accordingly, only two type of regional relationships are developed, which includes regional relationships considering explanatory variable as (i) catchment area only, and (ii) catchment and rainfall together. The coefficient of these regional relationships and corresponding coefficient of determination (R^2) are show in Table 3. It shows R^2 for regional relationships when only catchment area is considered as independent variable varying from 0.85 to 0.92. The R^2 for the regional relationship when both the explanatory variables i.e. catchment area (A) and catchment

Table 3: Regional relationship between dependable flows with basin area and catchment rainfall

Dependability	Relationship with area (A) $\{Q_e=a_1A^{a2}\}$			Relationship with area and rainfall $\{Q_e=a_1 A^{a2}P^{a3}\}$			
	Coefficients		R^2	Coefficients			R^2
	$\log a_1$	a_2		$\log a_1$	a_2	a_3	
10 %	0.34	0.89	0.92	-10.31	1.03	3.24	0.97
25%	0.24	0.88	0.90	-12.24	1.06	3.80	0.96
50%	0.10	0.89	0.90	-12.86	1.06	3.94	0.97
75%	-0.07	0.89	0.90	-13.37	1.07	4.04	0.98
90%	-0.12	0.85	0.85	-18.81	1.11	5.68	0.97

rainfall (P) are considered varied from 0.96 to 0.98. This shows that the relationships are better explained when both the explanatory variable are considered in the regional relationships. However, as a single independent variable catchment area (A) better explains the regional relationships. Results shows that the relationship has been improved with additional independent variable catchment rainfall. The validation (for five sites) is considered only for high flow (10% dependable flows) as some of the sites are seasonal. The R^2 value of 0.82 is estimated for the validation considering catchment area only.

6. CONCLUSIONS

The study discusses the three different methods of regionalization and argued that since most of the engineering planning and design requires information about water availability corresponding to some specific dependable flows such as 10%, 25%, 50 % 75%, 90%, regional relationships based on dependable flows provides an efficient way to estimates water availability rather than deriving the full flow duration curve. This saves additional computation efforts and can also be readily used for various design purposes. Results also show that as compared to relationships developed using only catchment area as independent variable, relationships having both catchment area and catchment rainfall as independent variable perform better.

REFERENCES

Archfield , S. A. et al. (2013), Topological and canonical kriging for design flood prediction in ungauged catchments: an improvement over a traditional regional regression approach? Hydrol.Earth. Syst. Sci 17, 1575-1588.

Barrows, H.K., (1943), Water Power Engineering: 3rd Ed., New York, McGraw-Hill Book Vo., 791 p.

Boscarello, L., Ravazzani, G., Cislaghi, A., & Mancini, M. (2015). Catchment classification for FDC regionalization.

Castellarin, A. et al., (2004), Regional flow duration curves: reliability for ungauged basins. Adv. Water Resour. 27, 953-965. http://dx.doi.org/10.1016/j.advwatres.2004.08.005.

Castellarin, A. et al., (2013), Rediction of flow duration curves in ungauged basins. In: BloschiG., et al. (Eds), Runoff prediction in ungauged basins: Synthesis Across Processes, Places and Scales, Cambridge University Press.

Castellarin, A., Galeati, G., Brandimarte, L., Montanari, A., & Brath, A. (2004). Regional flow-duration curves: reliability for ungauged basins. Advances in Water Resources.

Castellarin, S., Castellarin, A., Montanari, A., (2009), Prediction of low flow indices in ungauged basins through physiographical space based interpolation. Journal of hydrology, 378, 272-280.

Cheng, L., Yaeger, M., Viglione, A., et al. (2012). Exploring physical controls of regional patterns of flow duration curves. Hydrology and Earth System Sciences.

Chow, V.T., (1964), Handbook of applied hydrology. McGraw Hill Book Vo., New York, N.Y.

Claps, P., & Fiorentino, M. (1997). Probabilistic flow duration curves.

Cole, S. J., et al. (2011). Evaluation of regionalization approaches for FDCs.

Crocker, K., et al. (2003). Hydrological regional models.

CWC, (2014), Godavari Basin (Version 2.0), Central Water Commission, Ministry of Water Resources, Sewa Bhawan, R.K. Puram, New Delhi-110 066

CWC, (2018), Hydrological Data (Unclassified) Book, Information System Organization, Central Water Commission, New Delhi.

Demuth, S. (1993). Estimation of low flow characteristics.

Farmer et al. (2014), A comparison of methods to predict historial daily stream flow time series in southeastern United States (No. 2014-5231), U.S.G.S. Scientific Investigations Report.

Farmer, W.H., and Vogel, R.M., (2013), Performance-weighted methods for estimating monthly streamflow at ungauged sites: Journal of Hydrology, v. 477, p. 240–250, at http://dx.doi.org/10.1016/j.jhydrol.2012.11.032.

Fennessey, N. and Vogel, R. M., (1990), Regional flow duration curves for ungauged sites in Massachusetts, Journal of water resources planning and management, vol. 116, No.4, 530-549 pp.

Foster, H. A. (1934), Duration curves, Trans., ASCE, 99, 1213-1267

Ganora, D., Claps, P., Laio, F., & Viglione, A. (2009). Non-parametric FDC regionalization.

Gupta, R. S., (1889), Hydrology and hydraulic systems. Prentice-Hall, Inc., N.J., 363-367.
Hall, M., & Minns, A. (1999). Hydrologically homogeneous regions.
Hughes, D. A., & Smakhtin, V. (1996). Daily FDC applications.
Krasovskaia, I. et al., (2006), Regionalization of flow duration curves., Climate Variability and Change-Hydrological Impacts, Proceedings of the fifth FRIEND World Conference held at Havav, Cuba, November, 2006, IAHS Publ. 308.
Li, M., Shao, Q., Zhang, L., & Chiew, F. (2010). Regionalization approach for FDC.
Masih, I., et al. (2008). Regionalization using FDC similarity.
Mendicino, G., & Senatore, A. (2013). Parametric approaches for FDC regionalization.
Mimikou, R.. and Kaemaki, S., (1985), Regionalization of flow duration characteristics, Journal of Hydrology, 82, 77-91.
Olden, J. D., & Poff, N. L. (2003). Hydrologic indices and streamflow regimes.
Pessoa, F. C. L., et al. (2021). Regionalization of FDCs in large basins.
Pugliese A., et al., (2016), Regional flow duration curves: Geostatistical techniques versus multivariate regression, Advances in Water Resources, 9611-22.
Pugliese, A., et al. (2016). Geostatistical prediction of FDCs.
Riggs, H.C., (1982), Regional Analysis of Streamflow Characteristics (Chapter B3), USGS. Book 4, Hydrologic Analysis and Interpretation, 1-15pp.
Sadegh, M., Vrugt, J. A., Gupta, H. V., & Xu, C. (2016). Parametric models for FDC.
Searcy, J. K., (1959), Flow-Duration Curves, U.S. Geological Survey, Water Supply Paper, 1542-A, 33 pp.
Singh, K. P. (1971), Model flow duration and stream flow variability. Water Resource Research. 7, 1031-1036.
Tanase, I., & Petre, C. (2017). Regionalization of FDC for ungauged basins.
Vogel, R. M., & Fennessey, N. M. (1994). Flow duration curves: interpretation.
Wagener, T., Sivapalan, M., Troch, P., et al. (2007). Catchment classification and regionalization.
Yadav, M., Wagener, T., & Gupta, H. (2007). Regionalization in ungauged basins.
Ye, S., Yaeger, M., Coopersmith, E., et al. (2012). Physical controls of FDCs.

CHAPTER 2

REGIONAL FLOOD FREQUENCY ANALYSIS USING L MOMENTS

1 INTRODUCTION

Estimation of design flood is one of the important components of planning, design and operation of water resources projects. Information on flood magnitudes and their frequencies is needed for design of hydraulic structures such as dams, spillways, road and railway bridges, culverts, urban drainage systems, flood plain zoning, economic evaluation of flood protection projects etc. Pilgrim and Cordery (1992) mention that estimation of peak flows on small to medium-sized rural drainage basins is probably the most common application of flood estimation as well as being of greatest overall economic importance. In almost all cases, no observed data are available at the design site, and little time can be spent on the estimate, precluding use of other data in the region. Different methods have been used for estimating floods on small drainage basins. The three most widely used types of methods are the rational method, the U.S. Soil Conservation Service method and regional flood frequency methods. The choice of method depends on the design criteria applicable to the structure and availability of data. As per Indian design criteria, frequency based floods find their applications in estimation of design floods for almost all the types of hydraulic structures viz. small size dams, barrages, weirs, road and railway bridges, cross drainage structures, flood control structures etc., excluding large and intermediate size dams. For design of large and intermediate size dams probable maximum flood and standard project flood are adopted, respectively (NIH, 1992).

In India, a number of studies have been carried out for estimation of design floods for various structures by different organizations. Prominent among these include the studies carried out jointly by Central Water Commission (CWC), Research Designs and Standards Organization (RDSO) and India Meteorological Department (IMD) using the method based on synthetic unit hydrograph and design rainfall considering physiographic and meteorological characteristics for estimation of design floods (e.g. CWC, 1985) and regional flood frequency studies carried out by RDSO using the USGS and pooled curve methods (e.g. RDSO, 1991) for some of the hydrometeorological Subzones of India. But, most of the regional flood frequency analysis studies carried out in India are based on the conventional approaches. L-moments of a random variable were first introduced by Hosking (1986). Hosking and Wallis (1997) described the L-moments approach in regional frequency analysis. In the present study, regional flood frequency relationships have been developed, based on the L-moments approach for estimation of floods of various return periods for the gauged and ungauged catchments of the Lower Godavari basin subzone 3(f).

2 LITERATURE REVIEW

Regional Flood Frequency Analysis (RFFA) using L-moments has become a widely accepted approach for estimating design floods, particularly in ungauged or data-scarce basins. L-moments, defined as linear combinations of order statistics, provide reliable measures of variability, skewness, and kurtosis, and are less sensitive to outliers compared to conventional moments (Hosking, 1990). Over the period, extensive research has highlighted the effectiveness of L-moment-based techniques in improving the reliability of regional flood estimation.

A critical step in RFFA is the identification of homogeneous regions. The framework developed by Hosking and Wallis (1997) has been widely applied, incorporating statistical measures such as discordancy and heterogeneity to ensure regional consistency. Several studies have successfully utilized this approach in diverse hydrological settings. For example, Yang et al. (2010) demonstrated the applicability of L-moments in capturing spatial variability in large river basins. Similarly, Aydogan et al. (2016) and Alam et al. (2016) reported that L-moment-based methods provide more consistent and reliable regionalization results compared to traditional moment-based approaches.

Another important aspect of L-moment-based RFFA is the selection of suitable probability distributions. L-moment ratio diagrams are commonly used to identify appropriate distributions such as the Generalized Extreme Value (GEV), Generalized Pareto (GPA), and Generalized Logistic (GLO) distributions. Drissia et al. (2019) observed that the suitability of these distributions depends on regional hydrological characteristics, with GPA and GLO often providing better fits in certain conditions. Supporting studies conducted in various climatic regions, including semi-arid and monsoon-dominated basins, have also emphasized the robustness of L-moments in distribution selection and parameter estimation (Haddad et al., 2012; Saf, 2009).

The index flood method plays a central role in regional analysis, allowing normalization of flood data and development of regional growth curves. Cassalho et al. (2018) demonstrated that combining L-moments with the index flood approach significantly improves the accuracy of flood predictions. Furthermore, Hailegeorgis and Alfredsen (2017) showed that L-moment-based regional models effectively reduce uncertainty in ungauged basins by incorporating spatial variability into the analysis.

Recent developments have focused on integrating L-moment techniques with advanced statistical and computational approaches. Requena et al. (2017) and Lee and Kim (2019) explored hybrid methods combining L-moments with simulation and data-driven models, leading to improved flood estimation performance. Additionally, studies by Khan et al. (2010) and Mesbahzadeh et al. (2019) confirmed the applicability of L-moment-based RFFA in diverse hydrological conditions, including arid and developing regions. These advancements demonstrate the flexibility and robustness of L-moments in addressing complex hydrological challenges. Overall, the literature establishes that L-moment-based RFFA is a powerful and efficient tool for regional flood estimation. Its ability to ensure homogeneity, support appropriate distribution selection, and reduce uncertainty makes it highly valuable for hydrological design, flood risk assessment, and water resources planning (Hailegeorgis et al., 2017).

3 STUDY AREA AND DATA AVAILABILITY

The Lower Godavari Basin, situated in the downstream reaches of the Godavari River in Andhra Pradesh, India, extends approximately between latitudes 15°30′N to 17°00′N and longitudes 80°00′E to 82°30′E, covering the extensive Godavari delta before it drains into the Bay of

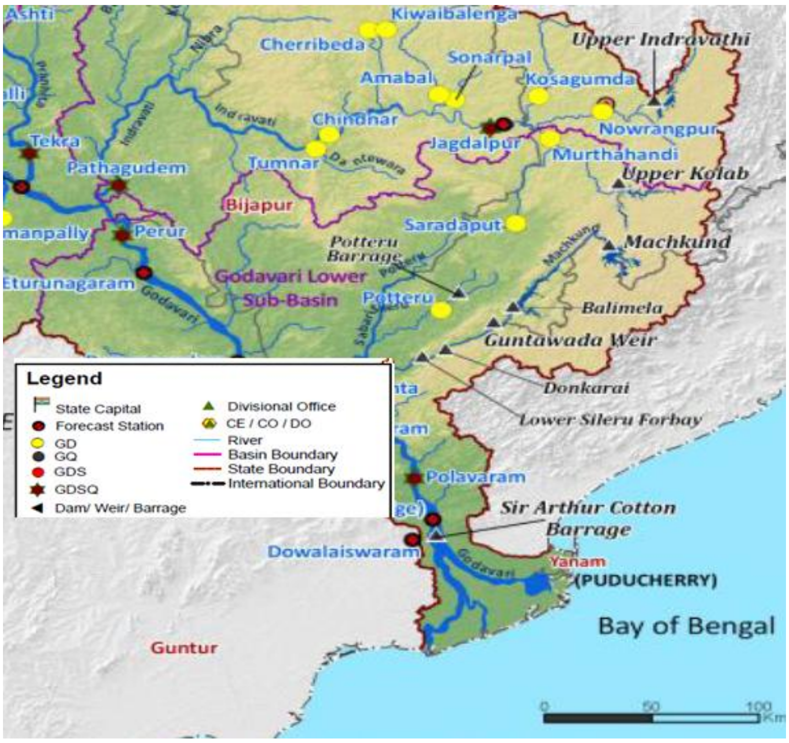

Fig 1: Lower Godavari Basin Subzone 3f

Bengal. The region is characterized by flat alluvial plains, fertile deltaic deposits, and a complex network of distributaries that support intensive agricultural activities. It experiences a tropical monsoon climate, with a mean annual rainfall of about 1000–1200 mm, most of which occurs during the southwest monsoon (June–September), along with additional contributions from northeast monsoon and cyclonic events. Due to its low-lying topography and coastal proximity, the basin is highly prone to flooding, storm surges, and cyclones. The hydrology of the basin is strongly influenced by upstream flows, reservoir operations, and monsoonal variability, making it an important region for flood frequency studies and water resources planning.

RDSO (1991) provides annual peak flood data varying over the period 1957 to 1989 for 115 bridge sites of the 7 hydrometeorologically homogeneous sub-zones of the 3. Accordingly, the area off each sub-zone, number of bridges sites for which data are available, range of catchment are of various bridge site, range of mean annual peak flood and record of length for various sub-zones are summarised in RDSO(1991). This information related to Sub-Zone 3f, Lower Godavari basin are as follows:

Table1: Salient features of sub-zone 3f Lower Godavari Basin

Subzone	**Area Km^2**	**No. of bridge sites**	**Range of catchment area (km^2)**	**Range of peak annual flood (m^3)**	**Range of record length (years)**
3f	174201	19	35.0 – 824.0	77.75-1212.83	14-29

This information has been updated based on the information available with CWC annual reports for Lower Godavari basin for further analysis. These has been detailed in Section 5.

4 METHODOLOGY: L-MOMENTS APPROACH

L-moments of a random variable were first introduced by Hosking (1986). They are analogous to the conventional moments, but are estimated as linear combinations of order statistics. Hosking and Wallis (1997) state that L-moments are an alternative system of describing the shapes of probability distributions. Historically they arose as modifications of the probability weighted moments' (PWMs) of Greenwood et al. (1979). In a wide range of hydrologic applications, L-moments provide simple and reasonably efficient estimators of characteristics of hydrologic data and of a distribution's parameters (Stedinger et al., 1992). The details of methodology for application of the L-moments approach in flood frequency analysis have been described by Hosking and Wallis (1997).

5 ANALYSIS AND DISCUSSION OF RESULTS

Screening of the data, testing of regional homogeneity, identification of the regional distribution and development of regional flood frequency relationships for gauged and ungauged catchments are described below.

5.1 Screening of Data using Discordancy Measure Test

The objective of the discordancy measure (D_i) test (Hosking and Wallis, 1997) is to identify those sites from a group of given sites that are grossly discordant with the group as a whole. Values of discordancy measure have been computed in terms of the L-moments for all the sites selected for Subzone 3(f). It is observed that the D_i values for all these sites are less than the critical D_i value of 2.757. Hence, as per the discordancy measure test, data of all the sites may be utilised for carrying out the flood frequency analysis. The details of each site and their L-moments and discordancy statistics are given in Table 2.

Table 2: L-Moments and discordancy measures

Stream Gauging Site	Catchment Area (km^2)	Mean Annual Peak Flood (m^3/s)	Sample Size (Years)	L-CV (τ_2)	L-skew (τ_3)	L-kurtosis (τ_4)	Discordancy Statistic (D_i)
184	364	344.48	29	0.3879	0.2106	0.1462	0.34
57	163	189.39	28	0.2567	0.1229	0.1154	1.02
973/1	362	505.04	28	0.3414	0.06	0.0323	0.6
912/1	137	404.86	29	0.4042	0.2779	0.1095	0.94
20	60	204.71	28	0.3335	0.0219	0.0529	1.02
4	50	237.97	29	0.2834	0.1236	0.0878	0.75
214	35	77.75	24	0.2813	0.246	0.2389	1.25
51	87	206.68	25	0.2802	0.0747	0.1428	1.35
807/1	824	1212.8	23	0.373	0.1823	0.0663	0.63
228	483	1075.3	22	0.3827	0.2806	0.1172	0.93
15	459	854.91	23	0.3767	0.1968	0.117	0.11
881/1	158	307.78	23	0.2855	0.0763	0.099	0.59
875/1	751	778.1	21	0.4119	0.0773	0.003	1.56
161	53	93.882	17	0.2992	0.3648	0.2329	2.03

36	139	170.8	15	0.415	0.3185	0.2357	1.43
224	750	687.36	14	0.4067	0.3365	0.2431	1.18
65	731	725.13	15	0.4147	0.4224	0.2557	1.27

The heterogeneity measure for Subzone 3(f) using available data at sites was computed and the same was found to be less than 1.0. Thus, the sites of the region comprising of 17 sites was identified as the homogenous region.

5.3 Identification of Regional Frequency Distribution

The choice of an appropriate frequency distribution for a homogeneous region is made by comparing the moments of the distributions to the average moments statistics from regional data. The aim of goodness-of-fit measure or the behaviour analysis is to identify a distribution that fits the observed data acceptably closely. The goodness of fit is judged by how well the L-Skewness and L-Kurtosis of the fitted distribution match the regional average L-Skewness and L-Kurtosis of the observed data. In this study, the L-moment ratio diagram and Z_i^{dist} have been used as goodness of fit measures for identifying the regional distribution. The L-moment ratio diagram based on approximations provided by Hosking (1991) has been used to identify the suitable regional flood frequency distribution. As shown in Fig. 2, the GEV distribution lies closest to the point defined by the regional average values of L-skewness and L-kurtosis, and the same is identified as the regional distribution.

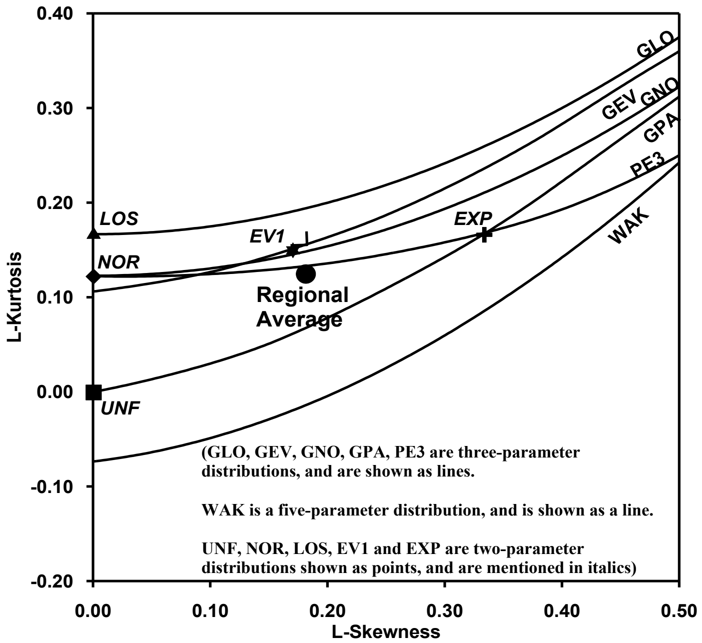

Fig 2: L moment ratio diagram for Lower Godavari Basin Sub-zone (3f)

Based on the Z^{dist} –statistic for the various three parameter it is observed that the Z^{dist} –statistic value is lowest for Pearson Type III (PE3), hence Pearson Type III (PE3) is the best fit distribution considering ZiDist statistics and L- Moments. Thus, the L-moment ratio diagram as well as Z^{dist} –statistic criteria ascertain that the PE3 distribution is the robust distribution for Subzone 3(f).

5.4 Development of Regional Flood Frequency Relationship for Gauged Catchments

As PE3 distribution has been identified the robust distribution for the study area; hence, regional flood frequency relationships have been developed using this distribution. The form of the regional frequency relationship for PE3 distribution is expressed as:

$$\frac{Q_T}{\overline{Q}} = u + \alpha\, y_T \qquad (1)$$

Here, Q_T is T-year return period flood estimate, u and α are the parameters of the PE3 distribution and Y_T is PE reduced variate corresponding to T-year return period i.e.

$$y_T = \left[1 - \left\{ -\ln\left(1 - \frac{1}{T}\right) \right\}^k \right] \Big/ k \qquad (2)$$

For estimation of flood of desired return period for a small to moderate size gauged catchment of Subzone 3(f), the above regional flood frequency relationship may be used. Alternatively, floods of various return periods may also be obtained by multiplying the mean annual peak flood of the catchment ($\overline{Q}$) by the corresponding value of growth factors given in Table 3.

Table 3: Values of growth factors ($Q_T/\overline{Q}$) for various distributions for Subzone 1(f)

Distribution	**Return Period**							
	2	**10**	**25**	**50**	**100**	**200**	**500**	**1000**
	Growth Factor							
PE3	0.89	1.85	2.31	2.64	2.95	3.26	3.66	3.96
GNO	0.89	1.83	2.31	2.67	3.02	3.38	3.87	4.24
GEV	0.89	1.83	2.32	2.68	3.05	3.42	3.92	4.30
WAK	0.90	1.84	2.31	2.64	2.96	3.28	3.67	3.95

5.5 Development of Regional Relationship between Mean Annual Peak Flood and Catchment Area

For estimation of T-year return period flood at a site, the estimate for mean annual peak flood is required. For ungauged catchments at-site mean can not be computed in absence of the observed flow data. In such a situation, a relationship between the mean annual peak flood of gauged catchments in the region and their pertinent physiographic and climatic characteristics is needed for estimation of the mean annual peak flood. As catchment areas (A) of the various bridge sites were the only physiographic characteristics available; hence, a regional relationship has been developed in terms of catchment area for estimation of mean annual peak flood ($\overline{Q}$) for ungauged catchments. This relationship is shown in Fig. 3 below:

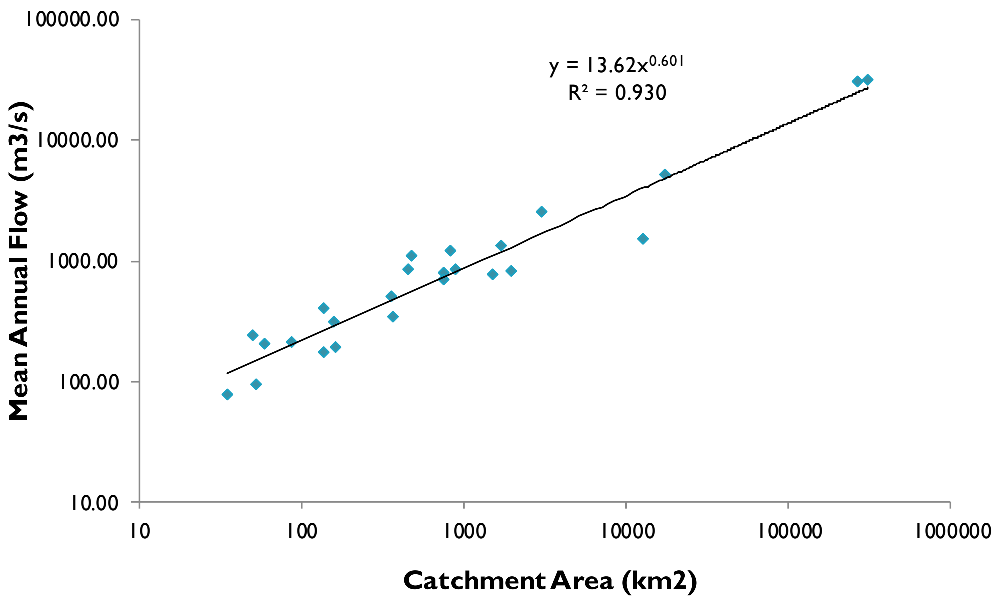

Fig 2: Relationship between catchment area and Q_{mean} for Lower Godavari Basin

The regional relationship between $\overline{Q}$ and A developed for the region as shown in Fig 3 using least squares approach (R^2=0.93) is given below.

$$\overline{Q} = 13.62\,(A)^{0.601} \tag{3}$$

Where, A is the catchment area, in km^2 and $\overline{Q}$ is the mean annual peak flood in m^3/s.

5.6 Development of Regional Flood Frequency Relationship for Ungauged Catchments

For development of regional flood frequency relationship for estimation of floods of various return periods for ungauged catchments, the regional flood frequency relationship given in equation (1) has been coupled with the regional relationship between mean annual peak flood and catchment area, given in equation (3) and following regional frequency relationship has been developed.

$$Q_T = [u + \alpha\, y_T] * 13.62 A^{0.601} \qquad (4)$$

Here, Q_T is flood estimate in m^3/s for T year return period, and A is catchment area in km^2, u and α are distribution parameters.

6 RAINFALL FREQUENCY ANALSIS

Extreme rainfall frequency analysis is critically important in hydrology and water resources management because it helps quantify the probability and magnitude of rare but high-impact rainfall events. By estimating return periods of extreme precipitation, this analysis supports the design of hydraulic structures such as dams, spillways, drainage systems, and urban stormwater networks, ensuring they can safely withstand intense storms. It also plays a vital role in flood risk assessment, disaster preparedness, and climate change adaptation by identifying trends and potential increases in rainfall extremes. Furthermore, extreme rainfall frequency analysis aids in developing early warning systems and sustainable land-use planning, thereby minimizing loss of life, infrastructure damage, and economic disruption in vulnerable regions.

In the study annual one-day maximum rainfall is used for rainfall frequency analysis. The gridded IMD data has been used to extract the annual one-day maximum rainfall in the lower Godavari basin at several gauging sites as shown in the Fig. below. The L-Moment statistics of these gauging sites are given in Table 5.

Fig: Grids in the Lower Godavari Basin

Table 5: L-Moment Statistics of annual one day maximum rainfall

Site Name	L-1	L-2	L-CV	L-skew	L-Kurt	Di (2.14)	CC
Ambabal	106.59	21.51	0.20	0.15	0.13	1.47	0.080 (<0.3)
Cherribeda	101.53	21.21	0.21	0.22	0.15	0.02	
Chindnar	96.42	18.52	0.19	0.23	0.17	0.00	
Perur	108.47	25.93	0.24	0.27	0.17	0.36	
Sangum	107.77	24.11	0.22	0.26	0.17	0.20	
Saradaput	122.67	27.44	0.22	0.27	0.17	0.37	
Sonarpal	105.54	23.07	0.22	0.2	0.17	0.21	
Tumnar	104.51	21.64	0.21	0.24	0.21	0.02	

The following frequency distribution are used for frequency analysis of one day maximum rainfall. Three statistical tests namely Kolmogorov-Smirnov (K-S Test), Anderson-Darling and Chi-Squared ($\chi 2$ Test) are used to test the fit statistics of five different distributions at 95%

confidence level (α = 0.05). The parameter of these distributions are shown in Table 6.

(i) **Generalised Extreme Value (GEV)**
(ii) **Generalised Logistic (GL)**
(iii) **Log-Pearson 3 (LP3)**

Table 6: Distribution and their parameters

Site Name	Distribution and their Parameters								
	Generalised Extreme Value (GEV)			Generalised Logistic (GL)			Log-Pearson 3 (LP3)		
	κ	σ	μ	κ	σ	μ	α	β	γ
Ambabal	-0.03	31.86	89.10	0.15	20.71	101.30	197.32	-0.03	9.73
Cherribeda	0.07	28.57	82.94	0.22	19.63	94.19	1008.50	0.01	-7.21
Chindnar	0.16	31.70	84.47	0.27	22.85	97.22	24.48	0.08	2.56
Perur	0.16	31.70	84.47	0.27	22.85	97.22	24.48	0.08	2.56
Sangum	0.14	30.11	85.68	0.26	21.49	97.74	22.60	0.08	2.77
Saradaput	0.15	33.72	97.34	0.27	24.25	110.88	25.39	0.08	2.79
Sonarpal	0.05	31.65	85.57	0.20	21.52	97.97	20854.00	0.00	-51.95
Tumnar	0.10	28.13	85.11	0.24	19.68	96.28	60.52	0.05	1.74

7 CONCLUSIONS

The regional flood frequency analysis based on L moment approach has been carried out for lower Godavari basin subzone 3f using L moment approach. The L moment approach ahs also been used for extreme rainfall frequency analysis in the basin. Based on the L-moment ratio diagram and Z^{dist} –statistic criteria; PE3 distribution has been identified as robust distribution for the study area. For estimation of floods of various return periods for gauged catchments of the study area, either the developed regional flood frequency relationship may be used or the mean annual peak flood of the catchment may be multiplied by corresponding values of the growth factors, computed using the PE3 distribution. For estimation of floods of desired return periods for ungauged catchments of the study area, the regional flood frequency relationship developed for ungauged catchments, its graphical representation or tabular form may be used.

As the regional flood frequency relationship have been developed using the data of catchments varying size in area; these relationships may be expected to provide estimates of floods of various return periods for the catchments of the Subzone 3 (f), lying nearly in the same range of areal extent, as those of the input data.The extreme rainfall frequency analysis has been carried out for annual one day maximum rainfall using L moment. The parameters of three distributions (GEV, GP, LP3) have been estimated, and their fit statistics have been estimated based on different fit criterion.

REFERENCES

Alam, J., Muzzammil, M. and Khan, M.K. (2016). Comparison of L-moment and conventional approaches. *ISH Journal of Hydraulic Engineering*.

Aydogan, D., Kankal, M. and Onsoy, H. (2016). Regional flood frequency analysis using L-moments. *Journal of Flood Risk Management*.

Cassalho, F., et al. (2018). Evaluation of L-moments based index flood procedure. *Hydrological Sciences Journal*.

Central Water Commission, 1985. Flood Estimation for Middle Ganga Plain Subzone 1(f). Report No. GP/10/1984, *Dte. of Hydrology (Small Catchments)*, New Delhi.

Drissia, T.K., Jothiprakash, V. and Anitha, A.B. (2019). Flood frequency analysis using L-moments. *Water Resources Management*.

Farquharson, J.R., 1992. Regional Flood Frequency Analysis in Arid and Semi Arid Areas. *Journal of Hydrology*, Vol. 138, pp 487-501.

Greenwood, J.A., Landwehr, J.M., Matalas, N.C. and Wallis, J.R., (1979). Probability weighted moments: Definition and relation to parameters of several distributions expressible in inverse form. Water Resources Research, 15, 1049-1054.

Haddad, K., Rahman, A. and Green, J. (2012). Regional flood frequency analysis using L-moments. *Journal of Hydrology*.

Hailegeorgis, T.T. and Alfredsen, K. (2017). Regional flood frequency analysis for ungauged basins. *Journal of Hydrology: Regional Studies*.

Hailegeorgis, T.T., et al. (2017). Uncertainty estimation in regional flood frequency analysis. *Hydrology Research*.

Hosking, J.R.M. (1990). L-moments: Analysis and estimation of distributions. *Journal of the Royal Statistical Society*.

Hosking, J.R.M. and Wallis, J.R. (1997). *Regional Frequency Analysis: An Approach Based on L-Moments*. Cambridge University Press.

Hosking, J.R.M. and Wallis, J.R., 1993. Some Statistics Useful in Regional Frequency Analysis. *Water Resour. Res.,* 29(6), pp 1745-1752.

Hosking, J.R.M. and Wallis, J.R., 1997. Regional Frequency Analysis-An Approach Based on L-moments. Cambridge University Press, N. Y.

Hosking, J.R.M., 1986. The Theorey of Probability Weighted Moments. *Res. Rep. RC12210,* IBM Res., Yorktown Heights, N.Y.

Hosking, J.R.M., 1990. L-moments: Analysis and Estimation of Distribution using Linear Combinations of Order Statistics. *J. R. Stat. Soc.,* SER. B, 52(1), pp 105-124.

Hosking, J.R.M., 1991. Approximations for Use in constructing L-moment ratio diagrams. *Res. Rep., RC-16635, 3,* IBM Res. Div., T.J., Watson Res. Cent., Yorktown Heights, N.Y.

Khan, M.S.R., et al. (2010). Regional flood frequency analysis using L-moments. *Applied Ecology and Environmental Research*.

Lee, D.H. and Kim, N.W. (2019). Regional flood frequency analysis using L-moments. *Water*.

Mesbahzadeh, T., et al. (2019). Flood frequency analysis in arid regions using L-moments. *Natural Resource Modeling*.

Natural Environmental Research Council, 1975. *Flood Studies Report*, Vol. I, Hydrological Studies, London.

RDSO (1991), Estimation of design discharge based on regional flood frequency approach for sub-zones 3(a), 3(b), 3(c) and 3€. Bridge and Floods Wing Report No. RGF-20.

Requena, A.I., Ouarda, T.B.M.J. and Chebana, F. (2017). Flood frequency analysis at ungauged sites. *Journal of Hydrometeorology*.

Research Design and Standards Organization., 1991. Estimation of Design Discharge Based on Regional Flood frequency Approach for Subzones 3(a), 3(b), 3(c) and 3(e). *Bridges and Floods Wing Report No. 20*, Lucknow.

Saf, B. (2009). Regional flood frequency analysis using L-moments. *Water Resources Management*.

Stedinger, J.R., Vogel, R.M., and Foufoula-Georgiou, E., 1992. Frequency Analysis of Extreme Events. In *Handbook of Hydrology*, edited by D.R. Maidment, Chapter 18, Mc Graw-Hill, N Y.

Vogel, R.M. and Fennessey, N.M., 1993. L-moment Diagrams Should Replace Product Moment Diagrams, *Water Resour. Res.,* 29(6), pp 1745-1752.

Yang, T., Xu, C.Y., Shao, Q. and Chen, X. (2010). Regional flood frequency analysis using L-moments. *Stochastic Environmental Research and Risk Assessment*.

CHAPTER 3

DEVELOPMENT OF REGIONAL RELATIONSHIPS FOR NASH AND CLARK IUH MODELS PARAMETERS

1 INTRODUCTION

For planning, development and operation of various water resources schemes estimation of runoff response from the ungauged catchments has been an important subject of research in the sphere of surface water hydrology. The conventional techniques of derivation of unit hydrograph (UH) require historical rainfall-runoff data. Due to the obvious reasons, adequate runoff data are not generally available for many of the small and medium size catchments. Indirect inferences through regionalisation are sought for such types of the ungauged catchments. Many times this task of regionalisation becomes very tedious and in certain cases even impossible. The research in the field of fluvial geomorphology has recently picked up and it offers some great opportunities in solving many of the problems facing the hydrologists today. As a first step in the direction of using geomorphologic characteristics with the conviction that the search for a theoretical coupling of quantitative geomorphology and hydrology is an area which will provide some of the most exiting and basic developments of hydrology in the future, the concept of geomorphologic instantaneous unit hydrograph (GIUH) was introduced by Rodriguez-Iturbe and Valdes (1979). The GIUH approach has many advantages over the regionalization techniques as it avoids the requirement of flow data and computations for the neighboring gauged catchments in the region as well as updating of the parameters. Another advantage of the GIUH approach is the potential of deriving the UH using only the information obtainable from topographic maps or remote sensing, possibly linked with geographic information system (GIS) and digital elevation model (DEM). Further, Bhaskar et al. (1997) mention that global atmospheric changes have been responsible for bringing about changes in rainfall patterns. In addition to these, land use changes within the catchment can have significant impact on runoff characteristics. Thus linking of the geomorphologic parameters with the hydrologic characteristics of the basin can provide a simple way to understand the hydrologic behavior of different catchments, particularly the ungauged ones. The objectives of the present study are (i) to derive GIUH from the geomorphological characteristics of a catchment by relating the GIUH to the parameters of the Clark instantaneous unit hydrograph (IUH) model (Clark 1945) for deriving its complete shape, (ii) to evaluate the geomorphological characteristics of the catchment required for derivation of the GIUH by employing GIS, and (iii) to compare the observed and simulated flood events using the GIUH based Clark model, the Clark IUH option of the HEC-1 package (HEC-1 1990) as well as the original Nash IUH model (Nash 1957) for evaluating the performance of the GIUH approach.

2 LITERATURE REVIEW

The GIUH theory was introduced by Rodriguez-Iturbe and Valdes (1979) by relating IUH peak and time to peak with geomorphologic characteristics of the catchment and a dynamic parameter velocity. In the GIUH based approach, a unifying synthesis of the hydrological response of a catchment to surface runoff was attempted by linking IUH with the geomorphological parameters of a catchment. Equations of general character were derived which express the IUH as a function of Horton's order ratios (Horton 1945). The expressions were given as:

$$q_p = 1.31 \ R_L^{0.43} \ V / L_\Omega \tag{1}$$

$$t_p = 0.44 \ (L_\Omega / V)(R_B / R_A)^{0.55} (R_L)^{-0.38} \tag{2}$$

where q_p = peak flow in units of inverse h, t_p = time to peak in h, R_B = bifurcation ratio, R_L = length ratio and R_A = area ratio given by the Horton's laws of stream numbers, lengths and areas respectively (Horton 1945), L_Ω = length in km of the highest order stream, and V = dynamic parameter velocity in m/s. On multiplying eq. (1) and (2) a non-dimensional term $q_p * t_p$ as mentioned below is obtained.

$$q_p * t_p = 0.5764 \ (R_B / R_A)^{0.55} (R_L)^{0.05} \tag{3}$$

The term $q_p * t_p$ is not dependent on the velocity and thereby on the storm characteristics and hence it is a function of only the geomorphological characteristics of the catchment. In the derivation of GIUH one of the difficulties involved is the estimation of peak velocity. This is a parameter that must be evaluated for each flood event. Rodriguez-Iturbe et al. (1982) rationalized that velocity must be a function of the effective rainfall intensity and duration and proceeded to eliminate velocity from the results. It leads to the development of geomorphoclimatic instantaneous unit hydrograph. The governing equations consist of the terms such as the mean effective rainfall intensity, Manning's roughness coefficient, average width and slope of the highest order stream. Rosso (1984) related the Horton's order ratios to the parameters of Nash IUH model on the basis of geomrphologic model catchment response. Rosso derived the parameters of Nash IUH model through power regression. Zelazinski (1986) gave a procedure for estimating the flow velocity which involves development of a relationship between the velocity and corresponding peak discharge. A methodology based on trial and error procedures has been suggested for estimating the maximum value of the velocity for each flood event. Bhaskar et al. (1997) derived the GIUH from the watershed geomorphological characteristics and then related it to the parameters of the Nash IUH model. Several studies have integrated GIUH with conceptual unit hydrograph models such as the Nash and Clark models to improve runoff prediction accuracy and parameter estimation. For instance, Sahoo and Saritha (2015) demonstrated the applicability of a GIUH-based Nash model for flood estimation in ungauged basins, achieving reliable simulation performance. Similarly, Bamufleh et al. (2020) developed a hybrid framework combining GIUH with both Clark and Nash models, highlighting improved hydrograph prediction through geomorphological parameterization. Earlier contributions by Adib et al. (2010) laid the foundation for incorporating GIUH into conceptual rainfall–runoff models, while Sabzevari and Noroozpour (2014) emphasized the role of basin geomorphology in enhancing model reliability. More recent advancements by Chen et al. (2019) further explored improvements in GIUH parameterization and its integration with established hydrological models. Collectively, these studies underline the importance of GIUH-based Clark and Nash models as robust tools for hydrological assessment, particularly in data-scarce regions.

The model parameters of the GIUH and the Nash IUH model were derived using two different approaches. In the first approach the rainfall intensity during each time interval is allowed to vary; whereas, in the second approach rainfall intensity is averaged over the entire storm period. In this study, the GIUH has been derived from the geomorphological characteristics of a catchment by relating the GIUH to the parameters of the Clark IUH model for deriving its complete shape.

3 METHODOLOGY

The subsections below explain the methodology

3.1 DEVELOPMENT OF GIUH BASED CLARK MODEL

The Clark IUH model is based on the concept that IUH can be derived by routing the unit excess-rainfall in the form of a time area diagram through a single linear reservoir. For the derivation of IUH the Clark model uses two parameters viz. time of concentration (T_c) in h and storage coefficient (R) in h, of a single linear reservoir in addition to the time-area diagram. The governing equation of the Clark IUH model is expressed as:

$$u_i = C\, I_i + (1-C)\, u_{i-1} \qquad (4)$$

where u_i = ith ordinate of the IUH, C and (1-C) = the routing coefficients, and C = Δt / (R + 0.5 Δt), Δt = computational interval in h, I_i = ith ordinate of the time-area diagram. A unit hydrograph of desired duration (D) may be derived using the following equation.

$$U_i = \frac{1}{n}(0.5\, u_{i-n} + u_{i-n} + u_{i-n+1} \ldots\ldots\ldots\ldots + u_{i-1} + 0.5\, u_i) \qquad (5)$$

where U_i = ith ordinate of unit hydrograph of D-hour duration and computational interval Δt hours, n = number of computational intervals in D-hours = D/Δt, and u_i = ith ordinate of the IUH.

Development of the GIUH based Clark model involves development of relationship between equilibrium velocity and excess-rainfall intensity and a procedure for derivation of unit hydrograph using the GIUH based Clark Model. Two approaches either of which may be applied based on the availability of river cross-sectional details of the ungauged catchment and the procedure developed for derivation of unit hydrograph using the GIUH based Clark model are as follows:

3.1.1 Relationship between Equilibrium Velocity and Excess-Rainfall Intensity - Approach-I

This approach may be utilized when the geometric properties of the cross-section of the gauging site are known and the value of Manning's roughness coefficient can be adopted with an adequate degree of accuracy. The steps involved in this approach are: (i) Compute cross-sectional area (A), wetted perimeter (P) and hydraulic radius (R) on the basis of cross-sectional details corresponding to different depths of flow. (ii) Assume the frictional slope to be equal to the bed slope of the channel. (iii) Choose an appropriate value of Manning's roughness coefficient (n) from the values given in literature (e.g. Chow, 1964) for various surface conditions of the channel. (iv) Compute the discharge (Q) using the Manning's formula corresponding to each depth. (v) Plot depth versus discharge and depth versus cross-sectional area curves. (vi) Compute the equilibrium discharge (Q_e) corresponding to an excess-rainfall intensity (i mm/h) using the relation:

$$Q_e = 0.2778 \; i \; A_c \qquad (6)$$

where A_c is catchment area in km^2. (vii) Compute the depth corresponding to the equilibrium discharge (Q_e) using the depth versus discharge curve. (viii) Compute the area corresponding to the depth computed at step (vii) using the depth versus area curve. (ix) Compute the velocity (V) by dividing the discharge (Q_e) by the area computed at step (viii). (x) Repeat steps (vi) to (ix) to find velocity with respect to different intensities of excess-rainfall (e.g., 1, 2, 3, 4 mm/hr etc.). (xi) Develop the relationship between velocity and excess-rainfall obtained at step (x) in the form: $V = a\, i^b$, using method of least squares. Here, a and b are the regression coefficients.

3.1.2 Relationship between Equilibrium Velocity and Excess-Rainfall Intensity - Approach-II

This approach is based on the assumption that the value of the Manning's roughness coefficient is not available but the velocities corresponding to discharges passing through the gauging section at different depths of water flow are known from the observations. This approach though requires information on discharges and velocities at the gauging site, but it does not necessarily mean that it can be applied for the gauged catchments only. For the ungauged catchments also, this information may be easily obtained by gauging the stream intermittently for all ranges of depth of flow. This type of information may be gathered without incurring much cost and effort. The steps involved in this approach are: (i) For different depths of flow the discharges and the corresponding velocities are known by observation. (ii) Let these velocities and discharges be the equilibrium velocities V_e and the corresponding equilibrium discharges Q_e. (iii) For these Q_e values, find the corresponding intensities of excess-rainfall (i) from the following expression:

$$i = Q_e / (0.2778\ A_c) \qquad (7)$$

(iv) From the pairs of such V_e and i develop the relationship between the equilibrium velocity and the excess-rainfall intensity in the form: $V_e = a\ i^b$, using method of least squares.

3.2 Derivation of Unit Hydrograph using the GIUH Based Clark Model

The steps involved in derivation of unit hydrograph of a specific duration using the GIUH based Clark model approach are: (i) Compute the excess-rainfall hyetograph either by uniform loss rate procedure or by Soil Conservation Service – curve number (SCS-CN) method ("Hydrology" 1985) or by any other suitable method. (ii) Estimate the peak velocity (V) for a given storm using the highest excess-rainfall utilizing the relationship between velocity and intensity of excess-rainfall (as explained above). (iii) Compute the time of concentration (T_c) using the equation:

$$T_c = 0.2778 L / V \qquad (8)$$

where L = length of the main channel, and V = the peak velocity in m/s. (iv) Using T_c, compute time-area diagram of the catchment at each computational time interval employing the non-dimensional relation between cumulative isochronal area and the percent time of travel. (v) Compute the peak discharge (q_p) of IUH given by equation (1). (vi) Compute the values of storage coefficient R, using a non-linear optimization procedure, so that peak of the IUH estimated by the Clark model is equal to q_p computed in Step (v). (vii) Compute IUH using the GIUH based Clark model with the help of final values of storage coefficient (R) as computed in the step (vi), time of concentration (T_c) and the time-area diagram. (viii) Compute the D-hour UH using the relationship between IUH and UH of D-hour. (ix) For estimation of DSRO hydrograph convolute the excess-rainfall hyetograph with the unit hydrograph obtained in Step (viii).

4 STUDY AREA

The GIUH based Clark model described in the previous section has been applied to the catchment defined by bridge number 807 of Lower Godavari basin lying in Central India. Its catchment area is 824.70 km^2 and length of main stream is 64.25 km. It receives most of its rainfall from the south-west monsoon during the four months of June to September. It is subhumid region having mean annual rainfall varying between 1000 mm to 1600 mm. The average annual temperature varies from 25^0 C to 27.5^0 C over the study area. The broad soil groups in the study area are red soils. The red soils are further classified into red sandy, red loamy, and red yellow soils. Black soils are classified as deep black, medium black and shallow black soils. More than 50% of the area is covered by forests and only 25% of the area is arable land.

5 GEOMORPHOLOGIC CHARACTERISTICS USING GIS

In application of the GIUH approach, some of the important geomorphological characteristics are required to be evaluated from the toposheets. It is extremely difficult to manually derive the geomorphological characteristics from toposheets. Thus, it discourages the users from adopting the GIUH approach. However, now a day's geographical information system (GIS) software (open source as well as commercial) are available for derivation of these characteristics in a simplified manner. In this study, the geomorphologic characteristics of the study area have been evaluated using the GIS software, as described below

The boundary of the catchment, stream network and contours have been mapped using DEM and digitized maps (in the scale of 1:50,000). Length of each stream is computed by default and stored in the table along with the order of each stream. The Strahler's ordering scheme was followed for ordering of the river network (Strahler 1957). Fig. 1 shows drainage network map of the study area for the six order streams of the catchment. Table 1 provides the geomorphological characteristics viz. stream numbers, length, average length and average areas for streams of various orders for the study area. The geomorphological parameters viz. R_B = 4.366, R_L = 1.664, R_A = 4.362 were computed graphically by plotting N_w, L_w, and A_w versus order of the streams and estimating slope of the best fit lines. In the present study, the length of the highest order i.e. the sixth order stream is measured as 3.027 km. As the total length of the main river is 64.25 km, hence, it has been considered appropriate to use the average length of the fifth and sixth order as L_Ω which is computed as 19.40 km. This is because the length of the sixth order stream is too small to govern the process of generation of runoff for this catchment and the significance of the mean length of the next highest order viz. fifth order streams needs to be account for

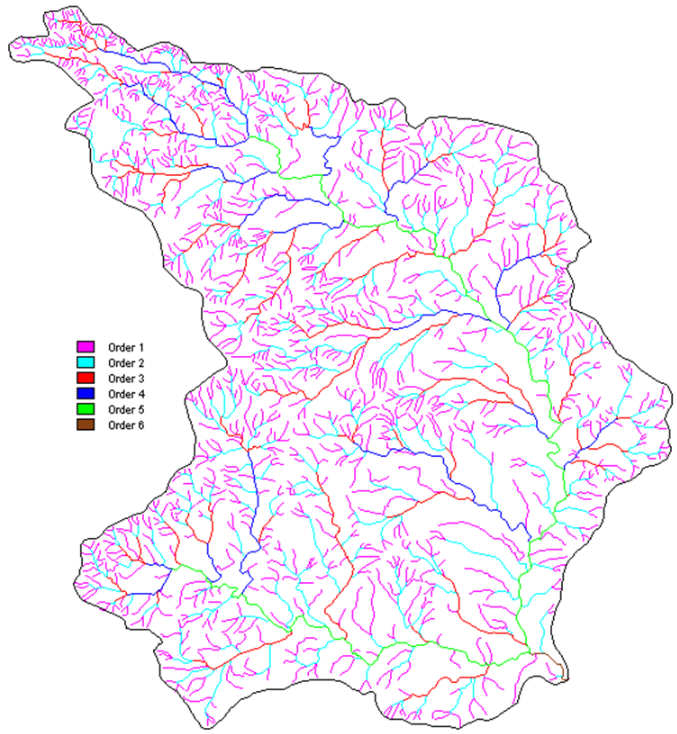

FIG. 1. Stream Network Map of the Catchment Defined by Bridge No. 807

TABLE 1. Geomorphological Characteristics of the Catchment defined by Bridge number 807 for Various Orders of Streams

Order of stream (1)	Total number of streams (2)	Total length of streams (km) (3)	Mean stream length (km) (4)	Mean Stream area (km^2) (5)
1	1163	893.100	0.768	0.520
2	299	347.300	1.162	2.272
3	63	179.200	2.844	9.916
4	18	96.372	5.353	43.284
5	2	71.557	35.778	188.930
6	1	3.027	3.027	824.700

For the catchment under study T_c is computed as 10 h. Using GIS, relative time of travel at various locations over the catchment was progressively computed, starting from the gauging site of the catchment. All the values of time of travels for each stream were then marked on the map of the catchment and these points were transferred in the digital form. Using interpolation technique a map of time distribution was drawn through these points. From the time distribution map values, a map at an interval of 1-h was prepared. For preparing time area diagram of the catchment, the area for each time interval was measured and these values were tabulated. Fig. 2 illustrates time area diagram of the study area.

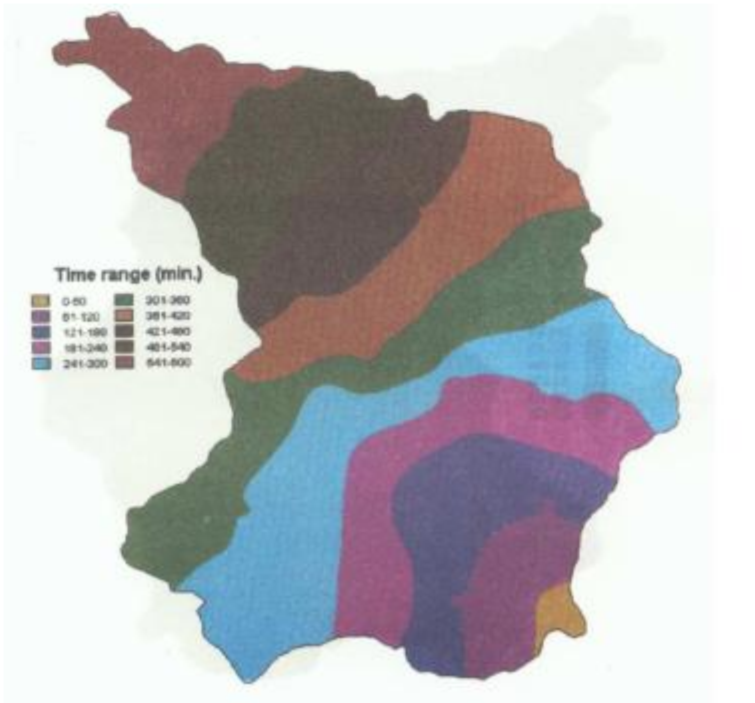

FIG. 2. Time Area Diagram of the Catchment Defined by Bridge No. 807

6 ANALYSIS AND DISCUSSION OF RESULTS

The DSRO hydrographs computed using the GIUH based Clark model have been compared with the observed DSRO hydrographs as well as with the DSRO hydrographs computed using the Clark IUH model option of the HEC-1 package and Nash IUH model. Some of the commonly used error functions have been evaluated for the GIUH based Clark model, HEC-1 package and the Nash IUH model based on the observed and the computed DSRO hydrographs. As the geometric properties of the gauging section and the value of Manning's roughness coefficient as well as the velocities corresponding to discharges passing through the gauging section at different depths of water flow were not available for the gauging site of the catchment under study, the two approaches of estimation of the velocity discussed above could not be applied in this study. Instead, the model was run by adopting the peak velocity of 2.75 m/s, which is based on the information obtained from the field engineers about the normally prevailing velocity at the gauging site, during the occurrence of the type of rainfall-runoff storms which have been considered in this study. The parameters of the Clark IUH model option of HEC-1 and the original Nash IUH model have been estimated using the historical data of all seven rainfall-runoff events by taking the geometric mean of the parameters derived for the remaining six out of the seven rainfall-runoff events each time by excluding the rainfall-runoff event whose excess-rainfall hyetograph has been used for convolution with the unit hydrograph and observed DSRO hydrograph has been used for comparing the computed DSRO hydrographs, derived by the aforementioned geometric mean parameter values. For example, the geometric mean values of the Clark and Nash IUH models for convolution with the excess-rainfall data of the first rainfall-runoff event have been computed by taking the geometric mean of the parameters derived for the nine rainfall-runoff events viz., Event No. 2 to Event No. 7; thus, excluding the parameter values obtained for the first event. The values of the parameters for all the seven individual rainfall-runoff events and the geometric mean parameter values for the original Clark and Nash IUH models derived from historical data are given in Table 2.

TABLE 2. Values of Parameters for Individual Storms and Mean Parameters for Clark and Nash IUH Models Derived from Historical Data

Event number	Clark model of IUH (HEC-1 package)				Nash IUH model			
	For individual storm		Geometric mean*		For individual storm		Geometric mean*	
	T_c	R	T_c	R	n	K	n	K
(1)	(2)	(3)	(4)	(5)	(6)	(7)	(8)	(9)
1	6.08	2.50	2.86	2.36	4.02	1.35	3.55	1.17
2	3.89	1.60	3.09	2.54	5.31	0.70	3.39	1.31
3	2.88	2.50	3.24	2.36	3.44	1.18	3.65	1.20
4	3.91	1.41	3.08	2.59	3.93	0.82	3.57	1.28
5	2.45	2.77	3.33	2.32	2.74	1.46	3.79	1.16
6	4.90	2.97	2.97	2.29	7.62	0.76	3.19	1.29
7	1.05	3.71	3.84	2.21	1.34	3.48	4.27	1.00

*Geometric mean values based of the parameters T_c and R of the remaining storms.

The values of R and T_c for the GIUH based Clark model have been estimated as 1.16 h and 6.49 h respectively. For the HEC-1 package the arithmetic mean values of R and T_c for the seven events are 2.49 h and 3.59 h and their standard deviations are 0.79 h and 1.65 h respectively. The lower and upper 95% confidence limits of R for the HEC-1 package are computed as 1.19 h and 3.79 h and lower and upper 95% confidence limit of T_c are computed as 0.88 h and 6.30 h respectively. The value of R for the GIUH based Clark model is well within 95% confidence limits and the value of T_c is quite close to the 95% confidence limits of Clark IUH model option of the HEC-1 package.

6.1 Comparison of Observed and Computed DSRO Hydrographs

The DSRO hydrographs computed by the GIUH based Clark model have been compared with the observed DSRO hydrographs as well as with the DSRO hydrographs computed by the Clark IUH model option of the HEC-1 package and the Nash IUH model as shown in Fig. 4 through Fig. 6. The values of peak discharge and time to peak of the DSRO hydrographs for the ten rainfall-runoff events are given in Table 3.

Table 3. Peak Discharge and Time to Peak of Observed and Computed DSRO Hydrographs for the Various Rainfall-Runoff Events

Event number	Observed		GIUH		HEC-1		NASH	
	Q_p (m^3/s)	T_p (h)	Q_p (m^3/s)	T_p (h)	Q_p (m^3/s)	T_p (h)	Q_p (m^3/s)	T_p (h)
(1)	(2)	(3)	(4)	(5)	(6)	(7)	(8)	(9)
1	360.3	7	460.5	6	492.5	3	450.4	4
2	543.8	6	419.0	8	405.9	5	381.4	7
3	478.3	5	486.4	8	474.6	6	461.7	7
4	324.5	5	258.4	6	267.6	3	240.2	5
5	402.1	4	389.6	6	413.2	3	371.6	5
6	247.0	8	265.7	11	301.5	8	278.2	9
7	1391.0	4	1546.4	6	1461.6	6	1507.0	7

6.2 Comparison of Error Functions Used for Evaluation of the Computed DSRO Hydrographs

The values of the errors functions computed for evaluation of the DSRO hydrographs for the GIUH based Clark model approach, HEC-1 package and the Nash IUH model viz. (i) efficiency (EFF), (ii) absolute average error (AAE), (iii) root mean square error (RMSE), (iv) average error in volume (AEV), (v) percentage error in peak (PEP) and (vi) percentage error in time to peak (PETP) are given in Table 4. It is observed that the values of EFF for the GIUH based Clark model are higher in two cases out of the seven rainfall-runoff events. The values of EFF for HEC-1 package are higher in case of one event; while the values of EFF for Nash IUH model are higher in case of four events. AAE, RMSE and PEP are lowest for two cases for the GIUH based Clark model. In general, it is observed that the values of AAE are comparable for the three methods. AEV is the lowest for the HEC-1 package for all the seven events.

TABLE 4. Error Functions Computed for DSRO Hydrographs Estimated by GIUH Based Clark Model, HEC-1 Package and Nash IUH Model for Various Rainfall-Runoff Events

Methods	Error functions for DSRO hydrographs					
	EFF	AAE	RMSE	AEV	PEP	PETP
(1)	(2)	(3)	(4)	(5)	(6)	(7)
Event 1						
GIUH	82.97	42.09	53.14	143.37	27.80	-14.29
HEC-1	-61.42	122.67	164.14	134.60	36.69	-57.14
NASH	59.80	65.07	82.72	142.66	25.00	-42.86
Event 2						
GIUH	68.70	73.37	99.11	159.57	-22.94	33.33

HEC-1	76.14	64.93	90.01	151.64	-25.36	-16.67
NASH	86.06	45.19	66.04	157.93	-29.86	16.67
Event 3						
GIUH	68.02	62.53	100.32	165.40	1.69	60.00
HEC-1	71.73	63.25	97.42	155.94	-0.77	20.00
NASH	90.28	32.38	60.43	164.36	-3.48	40.00
Event 4						
GIUH	29.10	88.53	99.53	133.01	-20.39	20.00
HEC-1	70.54	48.56	71.46	123.99	-17.54	-40.00
NASH	73.22	53.66	68.80	127.75	-26.00	0
Event 5						
GIUH	29.93	83.22	112.15	156.80	-3.13	50.00
HEC-1	68.40	59.96	81.48	148.11	2.76	-25.00
NASH	80.23	43.30	67.20	155.50	-7.59	25.00
Event 6						
GIUH	82.65	30.77	37.88	91.48	7.56	37.50
HEC-1	32.31	62.67	75.29	86.29	22.05	0
NASH	75.45	36.28	45.81	90.94	12.65	12.50
Event 7						
GIUH	-33.72	357.24	455.04	487.64	11.16	100.00
HEC-1	63.58	186.34	258.35	466.35	5.07	50.00
NASH	11.57	290.78	383.76	485.72	8.34	75.00

7 CONCLUSIONS

Based on this study, the following conclusions are drawn.

(i) The GIUH based approach presented in this study considers the catchment under study as ungauged and utilizes the geomorphological characteristics of the catchment for estimation of the parameters of the GIUH based Clark model. Comparison of the DSRO hydrographs estimated by the GIUH based Clark model with the observed DSRO hydrographs as well as with the DSRO hydrographs computed using the Clark IUH model option of the HEC-1 package and the Nash IUH model shows that the DSRO hydrographs are estimated reasonably well by the GIUH based Clark model.

(ii) Further studies may be carried out to examine the effects of using the velocity-excess rainfall intensity relationships of the nearby gauged catchments over the simulation results of various events of different catchments. Possibility of using a regional velocity-excess rainfall relationship may be investigated, as this regional relationship and the geormophological characteristics of the ungauged catchments of the region may be used for derivation of unit hydrographs of the ungauged catchments.

REFERENCES

Adib, A., et al. (2010). Development of GIUH-based rainfall–runoff models for ungauged watersheds.

Bamufleh, S., et al. (2020). Developing a geomorphological instantaneous unit hydrograph based on Clark and Nash models. Hydrological Sciences Journal.

Bhaskar, N.R., B.P. Parida and A.K. Nayak. (1997). "Flood estimation for ungauged catchments using the GIUH". *J. Water Resour. Plang. and Mgmt.* 123, 4, pp. 228-238.

Chen, X., et al. (2019). Advances in geomorphological IUH and its application in hydrological modeling.

Chow V. T. (Edited). (1964). " Hand book of Applied Hydrology" McGraw Hill Book Company, New York.

Clark, C.O.. (1945). "Storage and the unit hydrograph". *Transactions of the American Society of Civil Engineers* 110:1419-46.

Horton, R.E. (1945). "Erosional development of streams and their drainage basins: hydrophysical approach to quatntitative morphology." *Bull. Geo.. Soc. Am., 56, 275-370.*

Hydrologic Engineering Centre (1990). "HEC-1 "Flood Hydrograph Package," *Program Users Manual,* US Army Corps of Engineers, Davis, Calif.

Hydrology. (1985). *National Engineering Handbook*, Supplement A, Sect. 4, Chapter 10, Soil Conservation Service, USDA, Washington, D.C.

Nash, J.E., (1957). "The form of instantaneous unit hydrigraph." *Int. Assn. of Sci. and Hydrol., Pub.* 1, 45, 3, 114-121.

Rodriguez-Iturbe, I., and J.B. Valdes. (1979). "The geomorphologic structure of hydrologic response", *Water Resour. Res*., 15 (6), 1409-1420.

Rodriguez-Iturbe, I., M. Gonzalas Sonabria, and R.C. Bras. (1982). "The Geomorpho-climatic theory of the instantaneous unit hydrograph", *Water Resour. Res.*, 18 (4), 877-886.

Rosso Renzo. (1984). "Nash model relation to Horton order ratios". *Water Resour. Res.*, 20 (7), 914-920.

Sabzevari, T., and Noroozpour, S. (2014). Application of GIUH in rainfall–runoff modeling for ungauged basins.

Sahoo, B., and Saritha, P. G. (2015). Estimating floods from an ungauged river basin using GIUH-based Nash model. Springer.

Strahler, A.N. (1957). "Quantitative analysis of watershed geomorphology*", Trans. Am.Geophys. Union*, Vol.38, pp.913-920.

Zelazinski, J. (1986)." Application of the geomorphological instantaneous unit hydrograph theory to development of forecasting models in Poland", *Hydrol. Sci. Jour.*, 31,2,6.

CHAPTER 4

IMPACT OF CLIMATE CHANGE ON FLOOD ESTIMATES

1. INTRODUCTION

A projected warmer climate is expected to accelerate the hydrologic cycle, thus altering rainfall magnitude and resulting flood flows. It is expected that projected climate change results in warming, affecting the distribution and amount of precipitation, sea level rise and eventually both the runoff yield at different points combined with melting of glaciers will adversely affect the water balance in different parts of the world.

Global warming intensifying the occurrence of unprecedented hot spells and downpours faster than predicted by historical trends (Diffenbaugh, 2020; Seneviratne, 2012). Diffenbaugh (2020) mentioned that predictions that relied only on historical observations underestimated by about half the actual number of extremely hot days in Europe and East Asia, and the number of extremely wet days in the U.S., Europe and East Asia. The change in climate has occurred at a global scale, still its effects often vary from region to region. Moreover, rainfall distribution and trend analysis is being targeted by the climatologists, hydrologist and agriculturist to evaluate the influence of climate globally (Ghosh et al., 2009; Kampata et al., 2008). In recent past, number of climatic studies have been conducted to examine rainfall trend and variability over Indian region (Lal, 2001; Kumar et al., 2010). It is also revealed that trend and variability at large-scale may vary from regional scale (Barsugli et al., 2009; Bisht et al., 2017a; Raucher, 2011). The extreme climatic events in Himalayan region have also been studies by different authors (Rimi, et al. 2018; Ma et al. 2017; Wang et al. 2015). Rimi et al (2018) mentioned that anthropogenic climate change doubled the likelihood of the 2017 pre-monsoon extreme 6-day rainfall event at northeast Bangladesh and also showed that the magnitude of this contribution is sensitive to the climatological period in use. Wang et al. (2015) studied the Himalayan snowstorm of October 2014 resulted from the unusual merger of a tropical cyclone with an upper trough, and their collective changes and mentioned that climate warming have increased the odds for similar events.

Several recent studies have investigated the climate change impact on extreme precipitation and flood events (Qin and Lu 2014; Tabari, 2020; Hirabayashi, 2021). Qin and Lu (2014) mentioned that various GCMs and emission scenarios suggested different results. The study provides an insight into the flood risks and its uncertainty under future climate change conditions. Tabari (2020) show an intensification of extreme precipitation and flood events over all climate regions which increases as water availability increases from dry to wet regions. The present study also investigates the trends in annual maximum series and their significance at 95% confidence level. The study also attempted to investigate the relationship between ENSO phenomenon and AMS series. The subsequent sections provide a description of the study area, data used and different methods used to investigate the trends in AMS.

2. LITERATURE REVIEW

Climate change has increasingly been recognized as a key factor influencing extreme hydrological events, particularly annual maximum floods (AMF). The annual maximum flood series, defined as the highest discharge recorded in a given year, forms the basis for flood frequency analysis and hydraulic design. Traditionally, these analyses assumed stationarity, implying that statistical properties of floods remain constant over time. However, growing scientific evidence indicates that climate change is altering precipitation patterns, temperature regimes, and hydrological processes, thereby challenging this assumption and influencing the magnitude and occurrence of extreme floods.

One of the most significant impacts of climate change on AMF is linked to changes in precipitation characteristics. Rising global temperatures enhance the atmosphere's capacity to retain moisture, which in turn leads to more intense rainfall events. Such increases in rainfall intensity are closely associated with higher peak discharges and an elevated likelihood of extreme flooding. Several studies have demonstrated a clear relationship between intensification of precipitation extremes and increased flood magnitudes across different climatic regions (Allan and Soden, 2008; Westra et al., 2013). This effect is particularly pronounced in regions dominated by monsoonal or convective rainfall systems, where short-duration, high-intensity storms play a crucial role in flood generation.

Hydrological simulation studies further support the influence of climate change on annual maximum floods. By integrating climate model outputs with hydrological models, researchers have projected notable increases in peak flows under future climate scenarios. These projections indicate that high-return-period floods are likely to experience greater amplification compared to more frequent events, suggesting an escalation in extreme flood risk. Such findings have been consistently reported across different river basins, emphasizing the sensitivity of flood behavior to climatic drivers (Arnell and Gosling, 2016; Hirabayashi et al., 2013).

Temperature variations also contribute significantly to changes in flood regimes. In cold and mountainous regions, rising temperatures accelerate snowmelt processes, resulting in earlier and potentially more intense spring floods. In contrast, in tropical and semi-arid regions, higher temperatures may enhance evapotranspiration rates but can also intensify atmospheric instability, leading to extreme rainfall events and flash floods. Additionally, antecedent soil moisture conditions, which are influenced by both temperature and precipitation, play a critical role in determining runoff generation and peak discharge. These interactions highlight the complex and region-specific nature of climate change impacts on flood characteristics.

Recent extreme flood events provide practical evidence of these changing dynamics. Large-scale flood occurrences in Europe and Asia have been associated with unusually intense rainfall events, with scientific assessments suggesting that climate change has increased both their probability and severity. Such observations reinforce the growing consensus that climate change is already affecting flood regimes and is likely to intensify hydrological extremes in the future (Blöschl et al., 2017; IPCC, 2021).

Another critical implication of climate change is the introduction of non-stationarity in flood frequency analysis. Conventional methods rely on the assumption that past hydrological records are representative of future conditions. However, climate-induced changes introduce trends and variability in flood series, making traditional approaches less reliable. To address this issue, researchers have proposed non-stationary models that incorporate time-varying parameters or climate indices into flood frequency analysis (Milly et al., 2008; Merz et al., 2012). These approaches provide a more realistic representation of evolving flood risks under changing environmental conditions.

Despite considerable progress, significant uncertainties remain in quantifying the impact of climate change on annual maximum floods. These uncertainties arise from differences in climate model projections, variability in hydrological model structures, and limitations in observational datasets. Moreover, regional heterogeneity in climatic and catchment characteristics complicates the generalization of findings. Consequently, many studies advocate the use of multi-model ensembles and probabilistic frameworks to better capture the range of possible future outcomes.Existing literature clearly indicates that climate change is altering annual maximum flood behavior through multiple interconnected processes, including intensified precipitation, temperature-driven hydrological changes, and evolving catchment conditions. While both observational evidence and modeling studies point toward an increase in flood magnitude and frequency in many regions, uncertainties persist. Addressing these challenges requires the integration of climate science with advanced hydrological modeling and the adoption of non-stationary approaches for improved flood risk assessment.

3. STUDY AREA

Annual Maximum Flows (AMF) series of different gauging sites in the lower Godavari basin are considered for trend analysis. The location of lower Godavari basin is shown as in Fig.1 The elevation range varies between 107 m to 1372 m (from MSL).

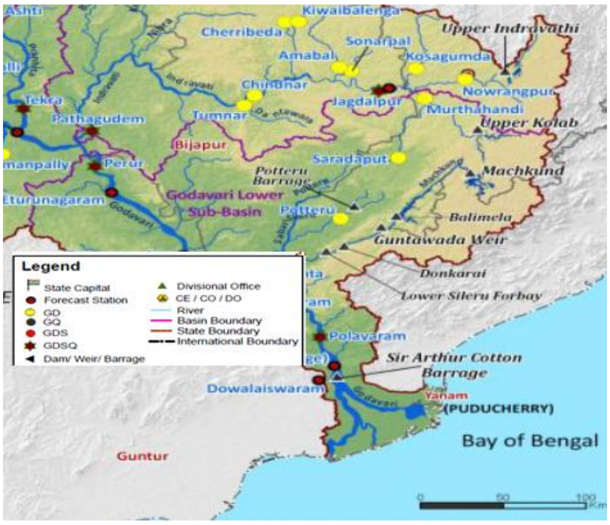

Fig. 1: Lower Godavari Basin

4. MATERIALS & METHODS

4.1 Data Used

The AMF series of five gauging sites are considering for trend analysis. The details of these sites and period of records available are show in Table 1. All these sites have AMF data for more than 40 years. The descriptive statistics of AMF time series at these five sites are also given in Table 1.

Table1: Descriptive statistics of AMF series at five stations

Site Name	Period (years)	Average	SD	CV	Skew
Chindnar	43	5169.20	2851.76	0.55	1.19
Perur	48	30675.35	13876.77	0.45	0.48
Polavaram	48	31506.85	12050.30	0.38	0.26
Saradaput	44	2550.70	1390.61	0.55	1.43
Somanpally	44	1503.15	1330.56	0.89	1.55

4.2 Trend Analysis

Spatio-temporal variability and investigation of AMF trends are essential input for climatic change impact on the frequency of floods disasters in a region. Trends in AMF series can be identified by using either parametric or non-parametric methods, and both the methods are widely used. The non-parametric methods do not require normality of time series and also are less sensitive to outliers and missing values. The non-parametric methods are extensively used for analyzing the trends in several hydrologic series namely rainfall, temperature, pan evaporation, wind speed etc .(Chattopadhyay et. al. 2011; Dinpashoh et. al. 2011; Fu et al. 2004;

Hirsch et al. 1982; Jhajharia and Singh 2011; Patra et al., 2012). The present study analyses the trends of AMF series of each individual station using non-parametric (Mann-Kendall test and Sens's estimator of slope) and parametric methods

4.3 Magnitude of trend using non-parametric method

The magnitude of trend in a time series was determined using a non-parametric method known as Sen's estimator (Sen 1968). This method assumes a linear trend in the time series and has been widely used for determining the magnitude of trend in hydro-meteorological time series (Lettenmaier et al. 1994; Partal & Kahya 2006). In this method, the slopes (T_i) of all data pairs are first calculated by

$$T_i = \frac{x_j - x_k}{j - k} \qquad \text{for i = 1,2,…,N} \qquad (2)$$

where x_j and x_k are data values at time j and k ($j > k$) respectively. The median of these N values of T_i is Sen's estimator of slope which is calculated as

$$\beta = \begin{cases} T_{\frac{N+1}{2}} & \text{if } N \text{ is odd,} \\ \frac{1}{2}\left(T_{\frac{N}{2}} + T_{\frac{N+2}{2}}\right) & \text{if } N \text{ is even.} \end{cases} \qquad (3)$$

A positive value of β indicates an upwards (increasing) trend and a negative value indicates a downwards (decreasing) trend in the time series.

4.4 Significance of trend

To ascertain the presence of a statistically significant trend in hydrologic climatic variables such as temperature, precipitation and streamflow with reference to climate change, the non-parametric Mann–Kendall (MK) test has been employed by a number of researchers (Douglas et al. 2000; Burn et al. 2004). The MK method searches for a trend in a time series without specifying whether the trend is linear or non-linear. The MK test checks the null hypothesis of no trend versus the alternative hypothesis of the existence of an increasing or decreasing trend. Following Bayazit & Onoz (2007), no pre-whitening of the data series was carried out as the sample size is large ($n \geq 50$) and slope of the trend was high (> 0.01).

The statistic S is defined as (Salas 1993):

$$S = \sum_{i=1}^{N-1} \sum_{j=i+1}^{N} \text{sgn}(x_j - x_i) \qquad (4)$$

where N is the number of data points. Assuming $(x_j - x_i) = \theta$, the value of sgn(θ) is computed as follows:

$$\text{sgn}(\theta) = \begin{cases} 1 & if \quad \theta > 0, \\ 0 & if \quad \theta = 0, \\ -1 & if \quad \theta < 0. \end{cases} \tag{5}$$

This statistic represents the number of positive differences minus the number of negative differences for all the differences considered. For large samples (N> 10), the test is conducted using a normal distribution (Helsel& Hirsch 1992) with the mean and the variance as follows:

$$E[S] = 0 \tag{6}$$

$$Var(S) = \frac{N(N-1)(2N+5) - \sum_{k=1}^{n} t_k (t_k - 1)(2t_k + 5)}{18} \tag{7}$$

where n is the number of tied (zero difference between compared values) groups and $t_k$is the number of data points in the kth tied group. The standard normal deviate (Z-statistics) is then computed as (Hirsch *et al.* 1993):

$$Z = \begin{cases} \frac{S-1}{\sqrt{Var(S)}} & if \quad S > 0 \\ 0 & if \quad S = 0 \\ \frac{S+1}{\sqrt{Var(S)}} & if \quad S < 0. \end{cases} \tag{7}$$

If the computed value of $|Z| > z_{\alpha/2}$, the null hypothesis H_0 is rejected at the α level of significance in a two-sided test. In this analysis, the null hypothesis was tested at 95% confidence level.

5. RESULTS AND DISCUSSIONS

Prior to non-parametric test, preliminary trend lines are fitted to the AMF values as shown in Fig 2, 3, 4, 5 & 6 and their results (slope and their significance)) are shown in Table 2. subsequently non- parametric statistical methods, Sen's estimator of slope (SE) and Mann–Kendall (MK) test have been carried out for estimating the magnitude and testing the statistical significance of trend (at confidence interval of 95%) respectively. However, prior to non-parametric test, data series was tested for presence of any auto-correlation. The outcomes of the analysis are shown in the form of Table 3.

Table 2: Preliminary trend line and its slope for AMF series of five gauging sites

Trend line (y=mx+c)					
S.N.	**Site Name**	**Trend (m)**	**t-Stat**	**Critical t value**	**Inference**

					(significance 95% level)
1	Chindnar	58.97	1.14	2.01	Not significant
2	Perur	-17.43	-0.12	2.01	Not significant
3	Polavaram	-29.06	-0.22	2.01	Not significant
4	Saradaput	-8.84	-0.53	2.01	Not significant
5	Somanpally	5.5	0.34	2.01	Not significant

Table 3: Sen slope (mm/year) for AMF series of five gauging sites

Site Name	Sen Slope	Z Statics	p-value	significance at 95%
Chindnar	38.76	105	0.27	non-significant
Perur	-16.05	-6	0.96	non-significant
Polavaram	-21.04	-26	0.82	non-significant
Saradaput	-7.91	-70	0.48	non-significant
Somanpally	-0.68	-2	0.99	non-significant

It is revealed from Table 2 and Table 3 that the AMF series of two gauging sites i.e. Chindnar and Somanpally having an increasing trend whereas three gauging sites i.e. Perur, Polavaram and Saradaput having decreasing trend. However, none of these trends are found to be significant at the 95% confidence level.

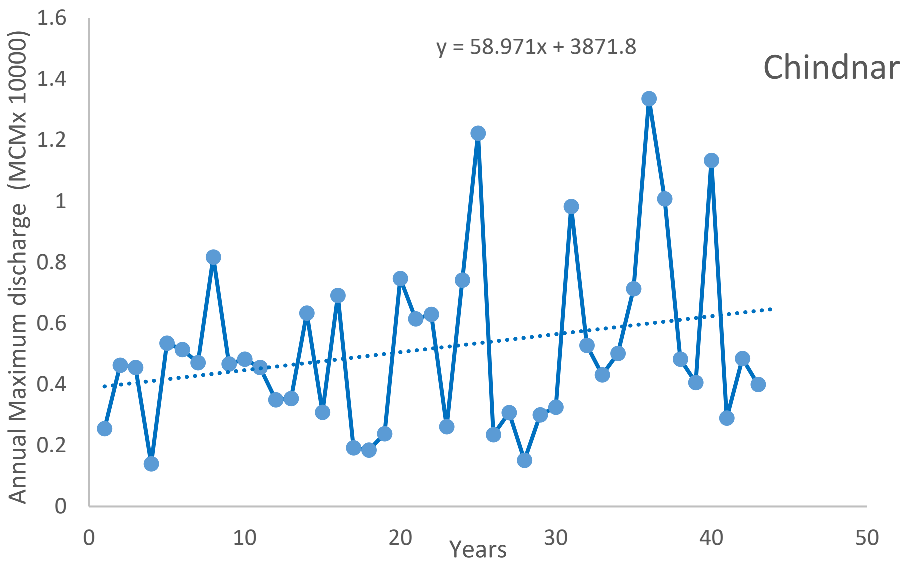

Fig.2: AMF series and trend line for Chindnar

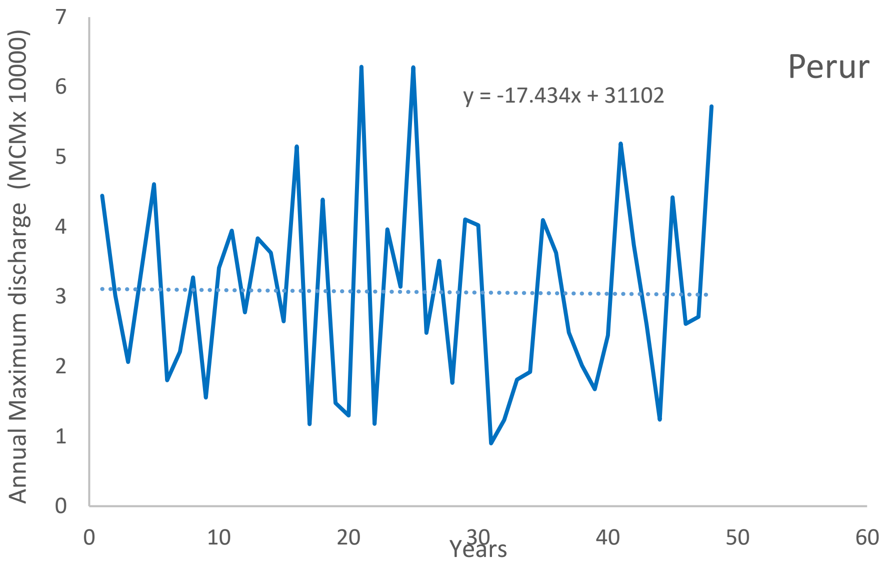

Fig.3: AMF series and trend line for Perur

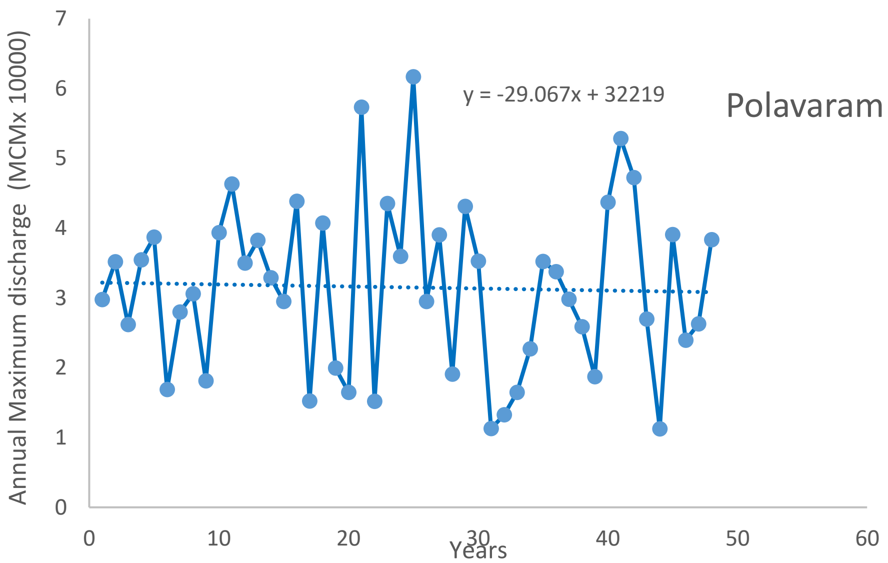

Fig.4: AMF series and trend line for Polavaram

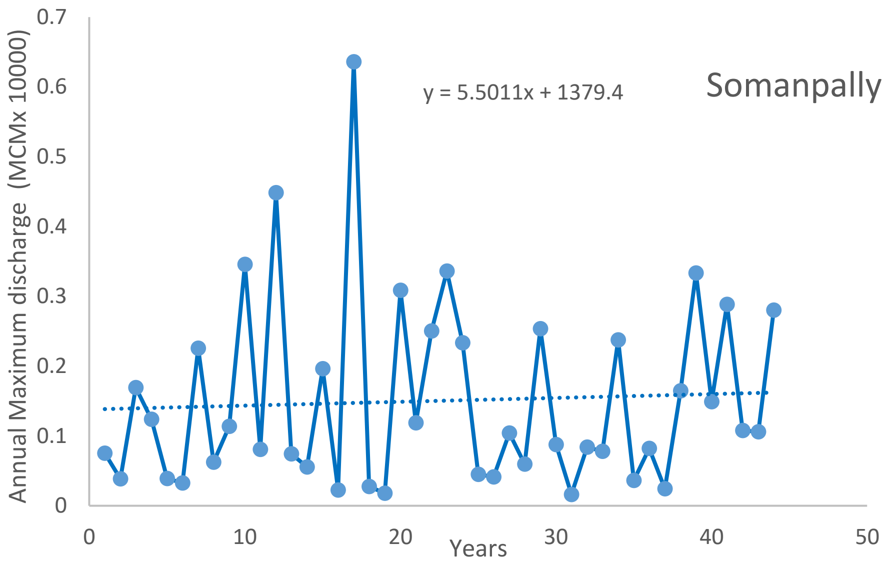

Fig.5: AMF series and trend line for Somanpally

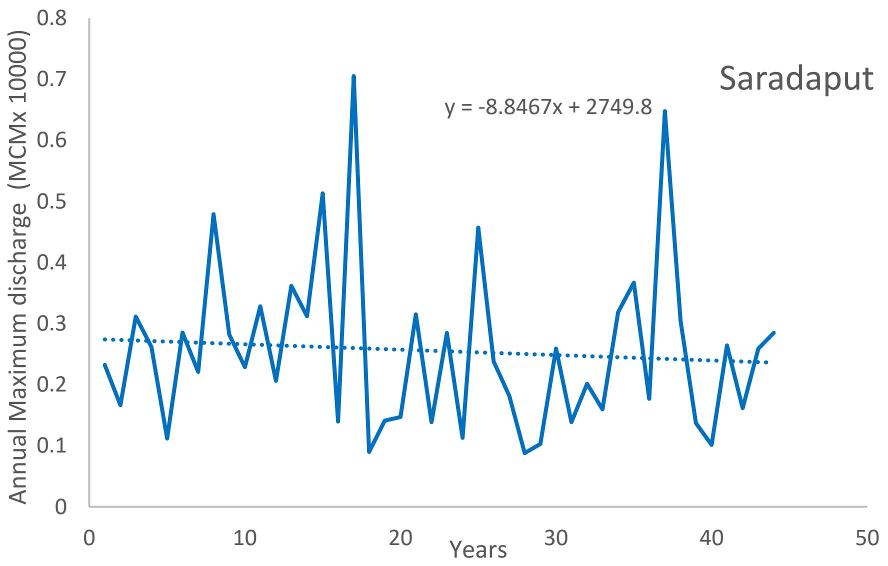

Fig.6: AMF series and trend line for Saradaput

6. RELATIONSHIP BETWEEN AMF AND EL NIÑO-SOUTHERN OSCILLATION (ENSO) PHENOMENON

Several studies from recent past have shown that Indian summer monsoon rainfall (ISMR) is influenced by El Nino-Southern Oscillation (ENSO) and several other low-frequency atmosphere-ocean oscillation including Pacific Decadal Oscillation (PDO), Arctic Oscillation (AO), etc. (e.g. Ashok et al., 2004; Dwivedi et al., 2015). Annual maximum flows or flood events in majority of the Indian watersheds result from the rainfall during monsoon period and so the effect of ENSO on ISMR is transferred to the watershed's extreme hydrology. Extreme hydrological events, including floods and droughts, across the globe are known to be impacted by these teleconnections (e.g. Gurrapu et al., 2016; Asong et al., 2018). In this context, a preliminary investigation has been carried out in this study to evaluate the influence of ENSO on annual maximum flows observed at selected flow gauging sites located along the Lower

Godavari Basin. The results indicate that the AMF in the selected gauging sites is significantly ($\alpha = 0.1$ or 90% confidence level), influenced by the phase of the ENSO phenomenon.

7. CONCLUSION

The study investigates the trends in the annual maximum flows at different gauging stations in the lower Godavari basin under climate change conditions. The study also attempted to examine the relationship between ENSO phenomenon and annual flood peaks. The results show that although all the five gauging sites showing either increasing or decreasing trends of annual maximum series however, these are not significant at 95% confidence level. The results of the parametric and non-parametric trend analysis are similar as none of the gauging station shows any significant trends at 95% confidence level. The examination of relationship between ENSO phenomenon and annual maximum flows shows that there is a positive relationship between two, however this needs further detailed investigation considering more information/ data about ENSO phenomenon in the study area.

REFERENCES

Allan, R. P., & Soden, B. J. (2008). Atmospheric warming and changes in precipitation extremes. Science.

Arnell, N. W., & Gosling, S. N. (2016). The impacts of climate change on river flows. Climatic Change.

Asong Z. E., Wheater H. S., Bonsal B., Razavi S. & Kurkute A. 2018 Historical drought patterns over Canada and their teleconnections with large-scale climate signals. *Hydrology and Earth System Sciences,* **22**(6), 3105-3124. https://doi.org/10.5194/hess-22-3105-2018

Barsugli J, Anderson C, Smith J B, and Vogel J M. 2009. Options for Improving Climate Modeling to assist water utility planning for climate change. *Water Utility Climate Alliance*, USA, 146 pp. Available from https://www.wucaonline.org/assets/pdf/pubs-whitepaper-120909.pdf

Bayazit M, and Önöz B. 2007. To prewhiten or not to prewhiten in trends analysis? *Hydrological Sciences Journal* **52** (4), 611-624. DOI: 10.1623/hysj.52.4.611

Bisht D S, Chatterjee C, Raghuwanshi N S, and Sridhar V. 2017. Spatio-temporal trends of rainfall across Indian river basins. *Theoretical and Applied Climatology* **132**, 419–436. DOI: 10.1007/s00704-017-2095-8

Blöschl, G., et al. (2017). Changing climate shifts timing of floods across Europe. Science.

Burn D H, Cunderlick J M, and Pietroniero A. 2011. Hydrological trends and variability in the Liard River Basin. *Hydrological Sciences Journal* **49** (1), 53-67. DOI: 10.1623/hysj.49.1.53.53994

Chattopadhyay S, Jhajharia D, and Chatopadhyay G. 2011. Univariate modelling of monthly maximum temperature time series over northeast India: neural network versus Yule-walker equation based approach. *Meteorological Applications* **18** (1), 70-82. DOI: 10.1002/met.211

Dankers, R., & Feyen, L. (2008). Climate change impact on flood hazard in Europe. Journal of Geophysical Research.

Diffenbaugh N S. 2020. Verification of extreme event attribution: Using out-of-sample observations to assess changes in probabilities of unprecedented events. *Science Advances* **6** (12), 2368. DOI: 10.1126/sciadv.aay2368

Dinpashoh Y, Jhajharia D, Fakheri-Fard A, Singh V P, and Kahya E. 2011. Trends in reference crop evapotranspiration over Iran. *Journal of Hydrology* **399** (3-4), 422-433. DOI: 10.1016/j.jhydrol.2011.01.021

Douglas E M, Vogel R M, and Kroll C N. 2000. Trends in floods and low flows in the United States: impact of spatial correlation. *Journal of Hydrology* **240** (1-2), 90–105. DOI: 10.1016/S0022-1694(00)00336-X

Fu G, Chen S, Liu C, and Shepard D. 2004. Hydro-climatic trends of the Yellow river basin for the last 50 years. *Climatic Change* **65**, 149-178. DOI: 10.1023/B:CLIM.0000037491.95395.bb

Ghosh S, Luniya V, and Gupta A. 2009. Trend analysis of Indian summer monsoon rainfall at different spatial scales. *Atmospheric Science Letters* **10** (4), 285–290. DOI: 10.1002/asl. 235

Gurrapu S., St-Jacques J. M., Sauchyn D. J. & Hodder K. R. 2016 The influence of the Pacific Decadal Oscillation on annual floods in the rivers of Western Canada. *Journal of the American Water Resources Association,* **52** (5), 1031-1045. DOI: 10.1111/1752-1688.12433

Hall, J., et al. (2014). Understanding flood risk under climate change. Nature Climate Change.

Hirabayashi Y, Alifu H, Yamazaki D, Imada Y, Shiogama H, and Kimura Y. 2021. Anthropogenic climate change has changed frequency of past flood during 2010-2013. *Progress in Earth and Planetary Science* **8,** 36. DOI: 10.1186/s40645-021-00431-w

Hirabayashi, Y., et al. (2013). Global flood risk under climate change. Nature Climate Change.

Hirsch R M, Slack J R, and Smith R A. 1982. Techniques of trend analysis for monthly water quality data. *Water Resources Research* **18** (1), 107-121. DOI: 10.1029/WR018i001p00107

IPCC (2014). Climate Change 2014: Impacts, Adaptation, and Vulnerability.

IPCC (2021). Climate Change 2021: The Physical Science Basis.

Jhajharia D, and Singh V P. 2011. Trends in temperature, diurnal temperature range and sunshine duration in Northern India. *International Journal of Climatology* **31** (9), 1353-1367. DOI: 10.1002/joc.2164

Kampata J M, Parida B P, and Moalafhi D B. 2008. Trend analysis of rainfall in the headstreams of the Zambezi River Basin in Zambia. *Physics and Chemistry of the Earth* **33** (8), 621–625. DOI: 10.1016/j.pce.2008.06.012

Kumar V, Jain S K, and Singh Y. 2010. Analysis of long-term rainfall trends in India. *Hydrological Sciences Journal* **55**, 484–496. DOI: 10.1080/02626667.2010.481373

Kundzewicz, Z. W., & Robson, A. (2004). Change detection in hydrological records.

Kundzewicz, Z. W., et al. (2014). Flood risk and climate change: global perspectives.

Kunkel, K. E., et al. (2013). Regional climate trends and extreme precipitation.

Lal M. 2001. Climatic change — Implications for India's water resources key sources of water in India. *Journal of Social and Economic Development* **3** (1), 57–97.

Lettenmaier D P, Wood E F, and Wallis J R. 1994. Hydro-climatological trends in the continental United States, 1948-88. *Journal of Climate* **7** (4), 586-607.

Ma S, Zhou T, Angélil O, and Shiogama H. 2017. Increased Chances of Drought in Southeastern Periphery of the Tibetan Plateau Induced by Anthropogenic Warming. *Journal of Climate* **30** (16), 6543–6560. DOI: 10.1175/JCLI-D-16-0636.1

Merz, B., et al. (2012). Flood frequency analysis under climate change.

Milly, P. C. D., et al. (2008). Stationarity is dead: Whither water management? Science.

Pall, P., et al. (2011). Anthropogenic greenhouse gas contribution to flood risk. Nature.

Partal T, and Kahya E. 2006. Trend analysis in Turkish precipitation data. *Hydrological Processes* **20**, 2011-2026. DOI: 10.1002/hyp.5993

Patra J P, Mishra A, Singh R, and Raghuwanshi N S. 2012. Detecting rainfall trends in twentieth century (1871-2006) over Odisha State, India. *Climate Change* **111**. 801-817. DOI: 10.1007/s10584-011-0215-5

Qin X S, and Lu Y. 2014. Study of Climate Change Impact on Flood Frequencies: A Combined Weather Generator and Hydrological Modeling Approach. *Journal of Hydrometeorology* **15** (3), 1205–1219. DOI: 10.1175/JHM-D-13-0126.1

Raucher, R.S., 2011. The Future of Research on Climate Change Impacts on Water: A Workshop Focusing on Adaptation Strategies. Water Research Foundation, 154 pp.

Rimi R, Haustein K, Barbour E J, and Allen M R. 2018. Risks of pre-monsoon extreme rainfall events of Bangladesh: Is anthropogenic climate change playing a role? *Bulletin of the American Meteorological Society* **100** (1), S61-S65. DOI: 10.1175/BAMS-D-18-0152.1

Sadegh, M., et al. (2016). Climate variability and flood extremes. Journal of Hydrology.

Seneviratne, S.I., N. Nicholls, D. Easterling, C.M. Goodess, S. Kanae, J. Kossin, Y. Luo, J. Marengo, K. McInnes, M. Rahimi, M. Reichstein, A. Sorteberg, C. Vera, and X. Zhang, 2012: Changes in climate extremes and their impacts on the natural physical environment. In: Managing the Risks of Extreme Events and Disasters to Advance Climate Change Adaptation [Field, C.B., V. Barros, T.F. Stocker, D. Qin, D.J. Dokken, K.L. Ebi, M.D. Mastrandrea, K.J. Mach, G.-K. Plattner, S.K. Allen, M. Tignor, and P.M. Midgley (eds.)]. A Special Report of Working Groups I and II of the Intergovernmental Panel on Climate Change (IPCC). Cambridge University Press, Cambridge, UK, and New York, NY, USA, pp. 109-230.

Tabari H. 2020 Climate change impact on flood and extreme precipitation increases with water availability. *Scientific Reports* **10,** 13768. DOI: 10.1038/s41598-020-70816-2

Trenberth, K. E. (2011). Changes in precipitation with climate change.

Wagener, T., et al. (2007). Catchment classification and hydrologic similarity.

Wang S-Y S, Gillies R R, Fosu B, and Singh P M. 2015. The deadly Himalayan snowstorm of October 2014: synoptic conditions and associated trends. *Bulletin of the American Meteorological Society*, **96** (12), S89–S94. DOI: 10.1175/BAMS-D-15-00113.1

Westra, S., et al. (2013). Future changes in precipitation extremes. Journal of Climate.

Zhang, X., et al. (2013). Detection of changes in precipitation extremes.

CHAPTER 5

CONCLUSIONS, CHALLEGNGES AND FUTURE PERSPECTIVES

1 CONCLUSIONS

The present study provides a comprehensive evaluation of regionalization techniques, flood frequency estimation, and extreme rainfall analysis with the objective of improving hydrological predictions for both gauged and ungauged catchments. The findings indicate that, in practical water resources planning and engineering design, estimating dependable flows (10%, 25%, 50%, 75%, and 90%) is often more efficient and directly applicable than constructing complete flow duration curves. Regional relationships developed for these dependable flows not only reduce computational complexity but also offer sufficient accuracy for planning purposes. Additionally, it was observed that models incorporating both catchment area and rainfall as predictor variables yield better performance compared to those relying solely on catchment area.

The application of the L-moment approach for regional flood frequency analysis in the Lower Godavari Basin (Subzone 3f) proved to be reliable and consistent. Based on L-moment ratio diagrams and Z-statistics, the Pearson Type III (PE3) distribution emerged as the most suitable probability distribution for the study region. The developed regional relationships enable the estimation of flood magnitudes corresponding to different return periods with reasonable confidence. For gauged catchments, flood quantiles can be obtained either directly from these relationships or by scaling the mean annual flood using growth factors derived from the PE3 distribution. In the case of ungauged catchments, the regional equations and their graphical or tabular representations provide a practical alternative for flood estimation.

It is important to note that the applicability of these regional relationships is most reliable when used within the range of catchment characteristics considered during their development. Since the dataset includes catchments of varying sizes, the relationships are expected to perform satisfactorily for hydrologically similar basins within the same subzone. Furthermore, the analysis of extreme rainfall using L-moments demonstrated that careful selection of probability distributions (such as GEV, GP, and LP3) based on goodness-of-fit measures is essential to obtain dependable design rainfall estimates.

The study also explored the use of the GIUH-based Clark model for simulating direct surface runoff hydrographs in ungauged basins. The results indicate that geomorphological characteristics can effectively be utilized to derive model parameters, and the simulated hydrographs show satisfactory agreement with observed data as well as outputs from established models like HEC-1 and Nash IUH. This highlights the usefulness of geomorphology-based approaches in regions where hydrological data is limited.

Trend analysis of annual maximum flows under changing climatic conditions revealed that, although certain stations exhibit increasing or decreasing tendencies, these trends are not statistically significant at the 95% confidence level. Both parametric and non-parametric approaches yielded consistent outcomes. Additionally, a positive association between ENSO events and flood peaks was observed; however, further investigation with more extensive datasets is required to better understand this relationship.

2 KEY CHALLENGES

Hydrological regionalization continues to face several important challenges that influence its reliability and applicability. One of the primary concerns is the limited availability of long-term, high-quality hydrological and meteorological data, particularly in ungauged or poorly monitored catchments. This data scarcity restricts the development of robust regional relationships and often introduces uncertainty in model predictions. In addition, significant variability in catchment characteristics—such as topography, land use, soil properties, and climatic conditions—makes it difficult to establish generalized relationships that are valid across diverse regions. Another major issue arises from uncertainties associated with the selection of appropriate probability distributions and parameter estimation techniques, especially when dealing with extreme hydrological events. Furthermore, the assumption of stationarity, which underpins many traditional hydrological methods, is increasingly challenged by climate change, as shifting precipitation patterns and temperature regimes alter hydrological responses over time. Ensuring reliable transfer of information from gauged to ungauged basins also remains a critical difficulty, as regional models may not fully capture local-scale variations.

3 FUTURE PERSPECTIVES

Considering above challenges, future research in regionalization should focus on developing more adaptive, data-rich, and robust methodologies. The integration of advanced data-driven approaches, including machine learning and hybrid modeling techniques, offers significant potential for improving prediction accuracy and capturing complex, nonlinear relationships among hydrological variables. There is also a growing need to move towards non-stationary modeling frameworks that explicitly account for the impacts of climate variability and long-term change. The use of remote sensing data and Geographic Information Systems (GIS) can help bridge data gaps and enhance spatial characterization of catchments, particularly in data-scarce regions. Additionally, improving techniques for transferring hydrological parameters between similar basins through better understanding of catchment similarity and scaling laws will enhance the reliability of predictions in ungauged areas. Strengthening the linkage between large-scale climatic drivers, such as ENSO, and regional hydrological responses is another important direction for future work. Finally, the development of standardized methodologies and guidelines for regionalization practices will promote consistency, comparability, and wider applicability of results across different studies and regions.